1/3/89

AD-A204 259

DTIC FILE COPY

REPORT DOCUMENTATION PAGE

1b. RESTRICTIVE MARKINGS

3. DISTRIBUTION / AVAILABILITY OF REPORT
See Distribution List

2b. DECLASSIFICATION / DOWNGRADING SCHEDULE

4. PERFORMING ORGANIZATION REPORT NUMBER(S)

5. MONITORING ORGANIZATION REPORT NUMBER(S)
AFOSR-TR- 89-0093

6a. NAME OF PERFORMING ORGANIZATION	6b. OFFICE SYMBOL (If applicable)	7a. NAME OF MONITORING ORGANIZATION
Regents of Univ. of Calif. Materials Department		AFOSR

6c. ADDRESS (City, State, and ZIP Code)	7b. ADDRESS (City, State, and ZIP Code)
College of Engineering University of California Santa Barbara, CA 93106	BF141 BAFB DC 20332-6448

8a. NAME OF FUNDING / SPONSORING ORGANIZATION	8b. OFFICE SYMBOL (If applicable)	9. PROCUREMENT INSTRUMENT IDENTIFICATION NUMBER
Air Force Office of Scientific Research	AFOSR/NE	AFOSR 88-0099

8c. ADDRESS (City, State, and ZIP Code)	10. SOURCE OF FUNDING NUMBERS			
	PROGRAM ELEMENT NO.	PROJECT NO.	TASK NO.	WORK UNIT ACCESSION NO.
AFOSR/NE Building 410 Bolling AFB DC 20332-6448	61102F	2305	C1	

11. TITLE (Include Security Classification)
High-Quality Three-Dimensional Electron Gases in Semiconductors

12. PERSONAL AUTHOR(S)
Dr. Arthur C. Gossard

13a. TYPE OF REPORT	13b. TIME COVERED	14. DATE OF REPORT (Year, Month, Day)	15. PAGE COUNT
Annual	FROM 1/1/88 TO 12/31/88	890103	70

16. SUPPLEMENTARY NOTATION

17. COSATI CODES			18. SUBJECT TERMS (Continue on reverse if necessary and identify by block number)
FIELD	GROUP	SUB-GROUP	Semiconductors, Three-Dimensional Electron Gases, Molecular Beam Epitaxy,

19. ABSTRACT (Continue on reverse if necessary and identify by block number)

As proposed, we have initiated an effort is begun to make high quality three-dimensional electron gases are made in semiconductors. ~~We are making~~ these structures by molecular beam epitaxy techniques using modulation doping to reduce impurity scattering and compositional grading techniques to control charge density profiles. We are collaborating with ~~the Westervelt and Halperin groups at~~ Harvard for high field and low temperature measurements and for search for electronic ordering phenomena. We are working with groups at Santa Barbara for probing the structures optically and looking for infrared frequency properties of the materials. Keywords:

DISTRIBUTION STATEMENT A
Approved for public release
Distribution Unlimited

20. DISTRIBUTION / AVAILABILITY OF ABSTRACT	21. ABSTRACT SECURITY CLASSIFICATION
☒ UNCLASSIFIED/UNLIMITED ☐ SAME AS RPT. ☐ DTIC USERS	Unclassified

22a. NAME OF RESPONSIBLE INDIVIDUAL	22b. TELEPHONE (Include Area Code)	22c. OFFICE SYMBOL
Dr. Gerald L. Witt, Program Manager	(202) 767-4931	AFOSR/NE

DD FORM 1473, 84 MAR — 83 APR edition may be used until exhausted. All other editions are obsolete. — SECURITY CLASSIFICATION OF THIS PAGE

805-961-2686

AFOSR-TR- 89-0093

January 3, 1989

SUBJECT: Annual Technical Report
Grant Nr. AFOSR-88-0099 (UCSB 08 148 88)
"High Quality Three-Dimensional Electron Gases in Semiconductors"

TO: Air Force Office of Scientific Research

ATTN: Dr. Gerald L. Witt
AFOSR
Bolling AFB, DC 20332

FROM: Professor Arthur C. Gossard
Materials and ECE Departments
University of California, Santa Barbara

Summary:

As proposed, we have initiated an effort to make high quality three-dimensional electron gases in semiconductors. We are making these structures by molecular beam epitaxy techniques using modulation doping to reduce impurity scattering and compositional grading techniques to control charge density profiles. We are collaborating with the Westervelt and Halperin groups at Harvard for high field and low temperature measurements and for search for electronic ordering phenomena. We are working with groups at Santa Barbara for probing the structures optically and looking for infrared frequency properties of the materials.

Work Statement:

In this research, we are exploring the production of high-quality three-dimensional electron systems of controlled density by growth of compostionally-graded, remotely-doped potential well structures. We will use computer-controlled molecular beam epitaxy to produce ultra-fine semiconductor superlattices with programmable composition gradients. We will produce conduction-band potential wells which are equivalent to the potential profiles of fixed pseudo-charge distributions but which are smoother than the spiked, strongly-scattering potential distributions associated with discrete dopant ions. We will introduce conduction electrons into the compositionally graded wells by remote doping of barrier regions. The electrons will distribute themselves in such a way as to screen the background potential and produce a uniform electrostatic potential and a uniform conduction electron charge distribution. We will also generate other potential profiles in order to create a range of additional carrier profiles. We will work originally with the GaAs/AlAs semiconductor system. One of the first uses of the structures to be grown under this proposal will be the search for predicted new ordered states of the electrons by collaborators at Harvard. We will use the results of the characterizations of the structures to further elucidate the molecular beam epitaxy process and we will examine possible uses of the three-dimensional electron gas in electronic and optical devices.

In pursuing this proposal, we will 1) develop procedures for the monitoring and computerized growth of precision graded-potential structures; 2) calculate and observe residual quantum effects in the structures; 3) electrically contact the structures and perform electrical and optical characterizations of them; 4) grow structures for observation of the predicted electronic ordering phenomena; and 5) grow structures for observation of additional new electronic phenomena and development of possible new device concepts.

Accomplishments:

1. The Santa Barbara molecular beam epitaxy laboratory is fully operational. Two new Varian Modular Gen II molecular beam epitaxy apparatuses have been set up and are growing semiconductor materials with state of the art electrical, optical and structural properties. Molecular beam fluxes have been calibrated with high speed ion gauge measurements. The modulation-doped

graded potential well structures needed for the three-dimensional electron gas are being grown under computer-control.

2. The band-bending and charge distributions expected in the three-dimensional electron structures have been modelled and calculated self-consistently. The results of this work, along with a report on the MBE growth and properties of the first samples, have been published in the paper, "Remotely-doped graded potential well structures", M. Sundaram, A. C. Gossard, J. H. English, and R. M. Westervelt, Superlattices and Microstructures 4, pp. 683-691 (1988). A copy of this paper is attached to this report. The interesting result of the simulations is that the carrier density in the central region of parabolically shaped potential wells is remarkably uniform and constant, even when the total doped carrier concentrations vary by over an order of magnitude. This is illustrated in Figure 1, which shows the computed carrier concentration profiles in a set of modulation-doped parabolic wells containing from one eighth to eight times the number of carriers needed to just fill the wells to a uniform carrier concentration.

3. More than two dozen successful structures have been grown. Structures were grown both for testing and calibration and for studies of the three dimensional electron gas. A typical layer structure and band diagram depicting the chief design parameters of interest are shown in Figure 2. The structural dimensions and compositions for a typical three dimensional electron gas sample, along with the carrier concentration and carrier mobility, are presented in Figure 3. Mobilities of up to $2X10^5$ cm^2/Vs (T=4.2K) were observed (the design parameters for this sample are given in Table 1), in spite of the presence of aluminum in the wells and forward and reverse heterostructure interfaces in the structures. Mobility vs temperature and concentration vs temperature plots for another typical sample, the structural parameters for which are presented in Table 2, are shown in Figure 4. Although these mobilities are not as high as in pure GaAs quantum wells and heterojunctions (in which alloy scattering is not present), they are amply high enough to observe magnetoquantum behavior and should be high enough to look for electron ordering phenomena like the predicted Celli-Mermin spin density wave formation.

4. Among the samples for testing were undoped graded structures, in which the potential profiles within the compositionally graded regions were examined by observations of photoluminescence

BAND DIAGRAMS AND ELECTRON DISTRIBUTION FOR DIFFERENT BARRIER DOPINGS:

T = 300K

Eq. Band Diagrams at diff. Barrier Dopings

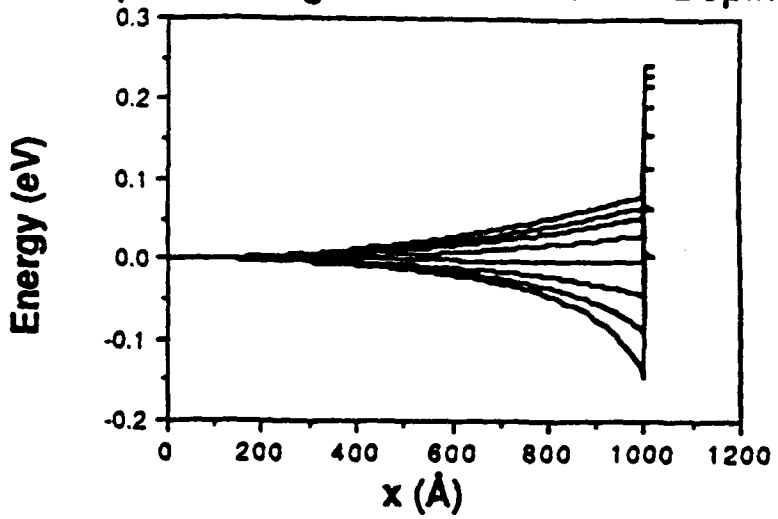

Eq. Electron Distributions at diff. Barrier Dopings

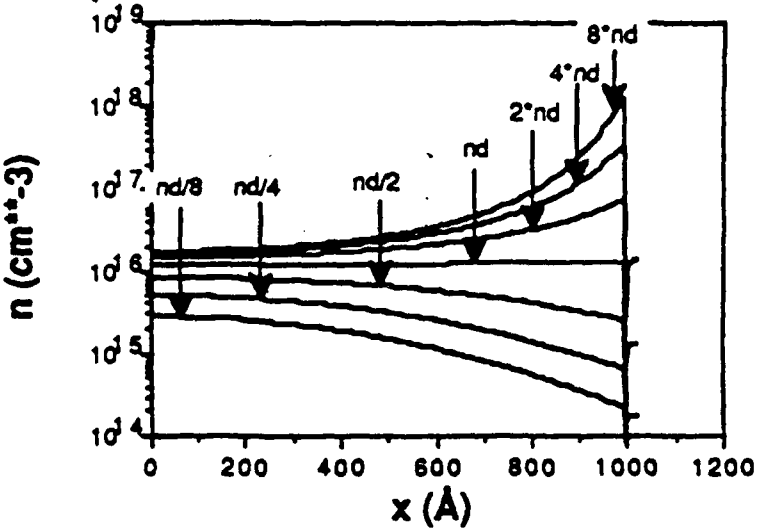

We see that the electron distribution remains approximately uniform over most of the well for a large range of barrier dopings, the excess or deficit being inserted or extracted from the well edges.

Fig. 1

Fig. 2

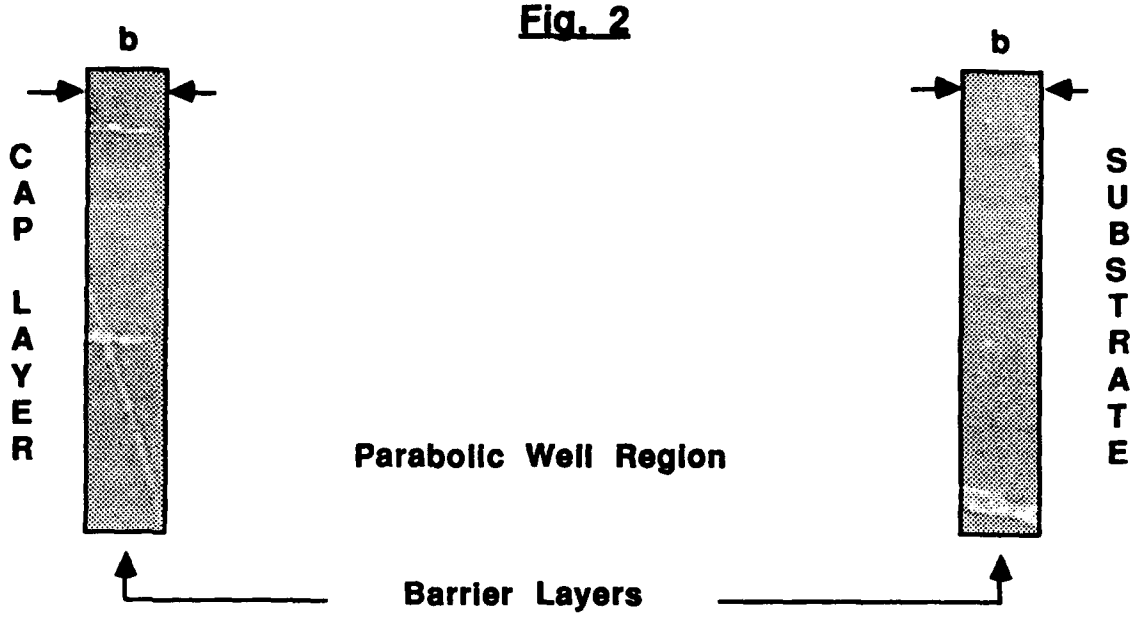

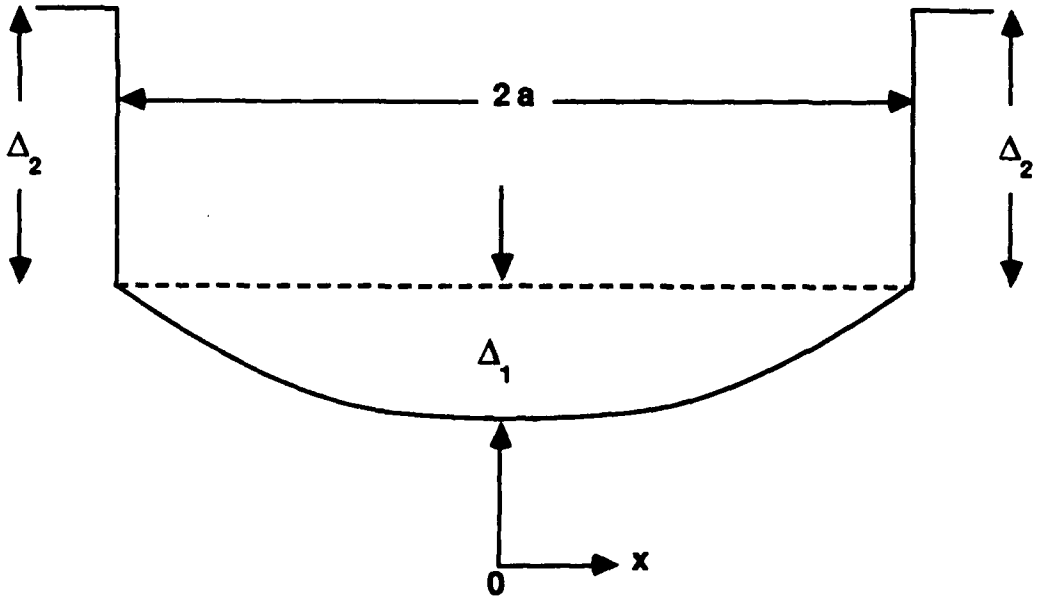

Layer structure and Band Diagram (assuming uniform permittivity and no doping) showing chief DESIGN PARAMETERS

TYPICAL PARABOLIC WELL STRUCTURE GROWN

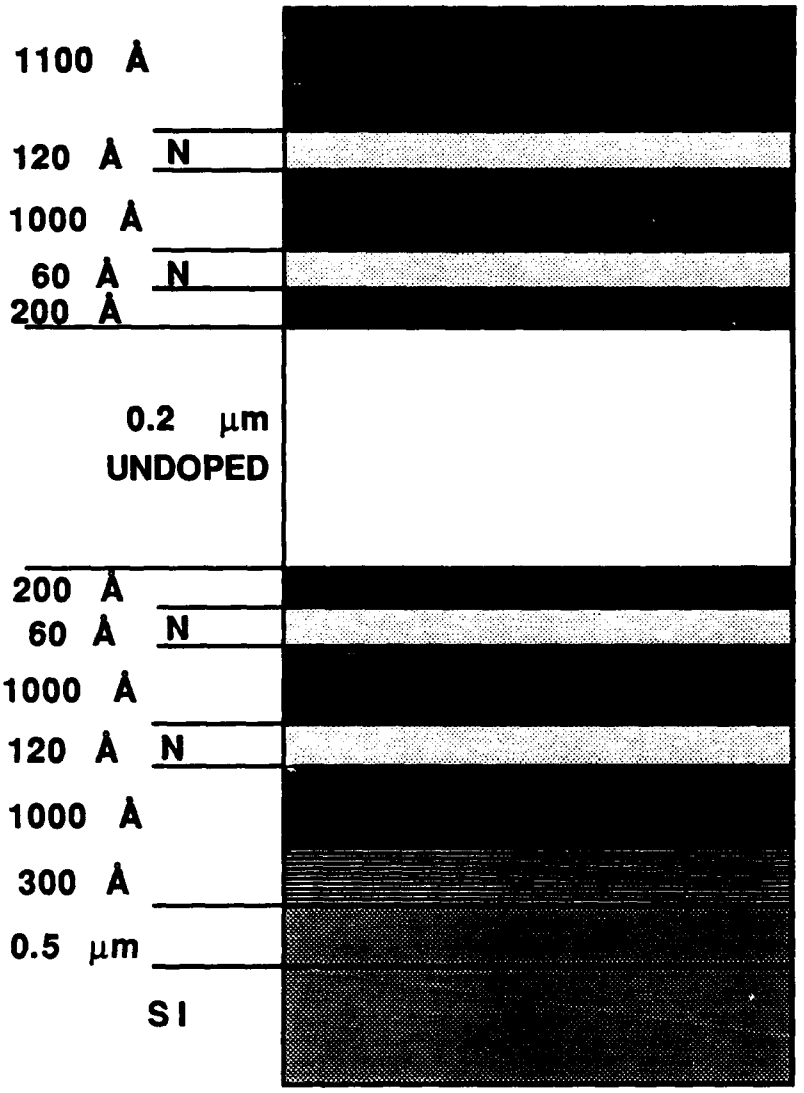

Outside the parabolic well, x in AlGaAs is 0.3

N = 5e17 cm^-3, DOPANT: Si

	μ(cm^2/Vs)	ns(cm^-2)	T(K)
	3951	5.38e11	300
BEST HALL MOBILITIES TO DATE:	5.6e4	2.58e11	77
	1.98e5	2.1e11	4.2(dark)
	2.04e5	2.12e11	4.2(light)

Fig. 3

TABLE 1

Structural parameters for sample 1

Parameter	Value
Δ_1	0.155eV
Δ_2	0.143eV
2a	2000Å
b	100Å
n_d	$2.1 \times 10^{17} cm^{-3}$
setback	200Å
$X_{Al\_well\text{-}centre}$	0
$X_{Al\_well\text{-}edge}$	0.2
$X_{Al\_barrier}$	0.4

Fig. 4

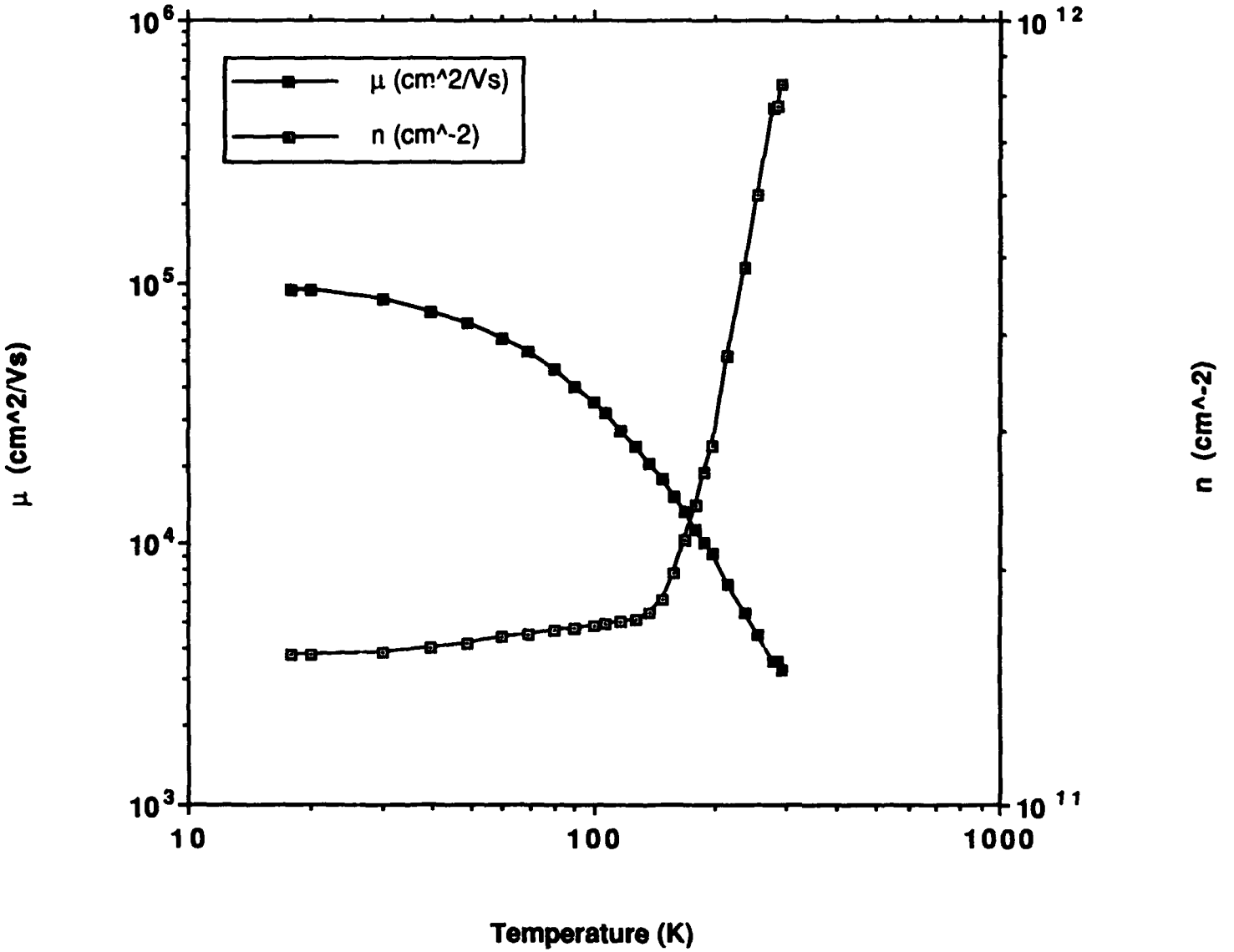
μ (cm^2/Vs)
n (cm^-2)
10^6
10^5
10^4
10^3
10^12
10^11
10
100
1000
μ (cm^2/Vs)
n (cm^-2)
Temperature (K)

TABLE 2

Structural parameters for sample 2

Parameter	Value
Δ_1	0.155eV
Δ_2	0.081eV
2a	2000Å
b	120Å
n_d	$5.0 \times 10^{17} cm^{-3}$
setback	200Å
$X_{Al\_well\text{-}centre}$	0
$X_{Al\_well\text{-}edge}$	0.2
$X_{Al\_barrier}$	0.3

and photoluminescence excitation spectroscopy in the laboratory of Professor James L. Merz and visiting researcher Dr. Perolaf Holtz. This principle is illustrated in Figure 5. An example of an excitation spectrum of a multilayer sample consisting of 10 parabolically shaped undoped quantum wells is shown in Figure 6. The uniform spacing of the principal transitions reflects the parabolic shape of the profile, while the sharpness of the spectral lines indicates the reproducibility of the wells. The widths of the wells must be equal to within approximately one part in 20 to produce such a spectrum.

5. Another set of samples was grown in order to study the charge distributions within the structures by means of capacitance measurements. These structures were modulation doped parabolic well structures grown on conducting substrates. The capacitance characteristics expected for electrons in graded composition structures were modeled by a computer calculation for comparison with the experimentally observed behavior. These calculations are the first computation of capacitance characteristics for graded modulation doped structures and appear to model the experimental results in a range of samples very successfully. For instance, Figure 7 shows the calculated actual electron profile and the apparent electron profile that would be observed in a CV measurement. Also shown is the doping profile, for a 2000 Å wide parabolic well (with a curvature corresponding to about 2e16 cm^{-3}) structure that is doped everywhere except in the well itself. Figure 8 shows a measured apparent profile and the recontructed fit, for such a design. Comparison with experiment shows that the symmetry of charge distributions in the potential wells can be strongly dependent on growth conditions. Growth methods involving superlattice buffer layers were then used which successfully avoided unwanted asymmetries in charge distributions. Figure 9 shows the measured and reconstructed profiles for a sample grown incorporating these changes. The calculations and experimental results for the capacitance behavior are being written in a paper which is in the final stages of preparation and which we will submit to the Journal of Applied Physics.

6. Approximately 4 different samples of modulation doped parabolic wells were sent to Harvard, where Professor Robert Westervelt and his students have made low temperature and high magnetic field measurements on them. They have observed the quantum Hall effect in these structures when several quantum subbands are occupied and have reported their findings at

PARABOLIC QUANTUM WELLS AS A MEANS OF GRADED PROFILE TESTING

LAYER STRUCTURE:

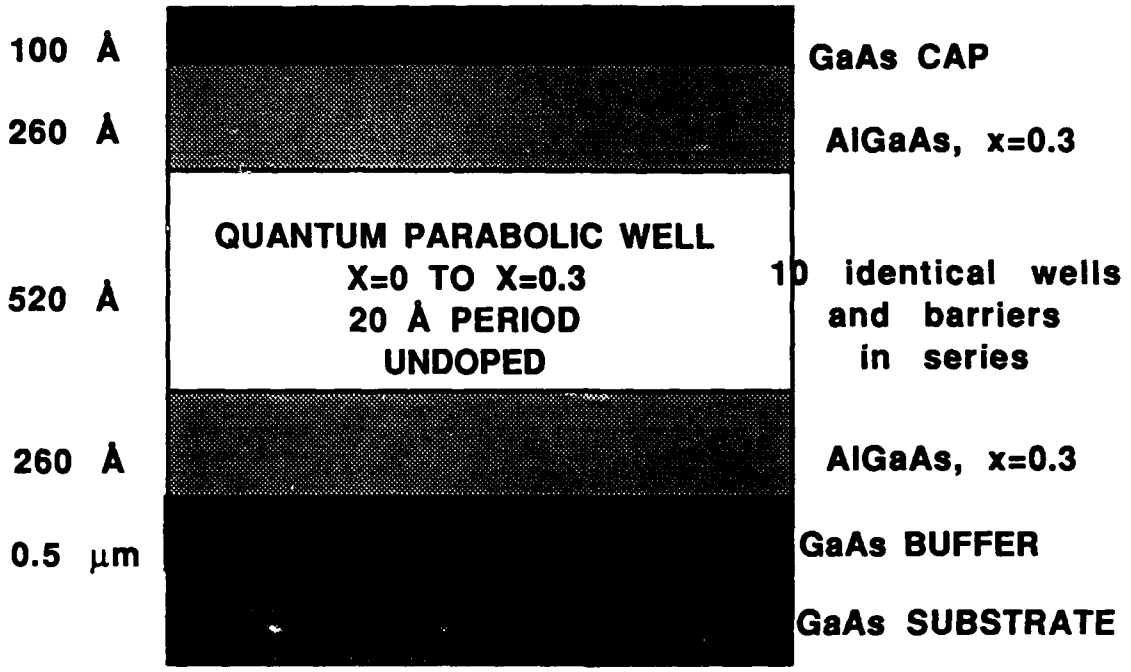

EXCITON TRANSITIONS EXPECTED TO BE OBSERVED IN A PHOTOLUMINESCENCE EXCITATION SPECTRUM

SOLID LINES IN VALENCE BAND ARE HEAVY HOLE STATES AND DOTTED LINES, LIGHT HOLE STATES

nh INDICATES A TRANSITION FROM THE n-th ELECTRON STATE TO THE n-th HEAVY HOLE STATE. OFF-DIAGONAL TRANSITIONS HAVING $\Delta n=2$, eg. 13h, ARE ALSO PREDICTED

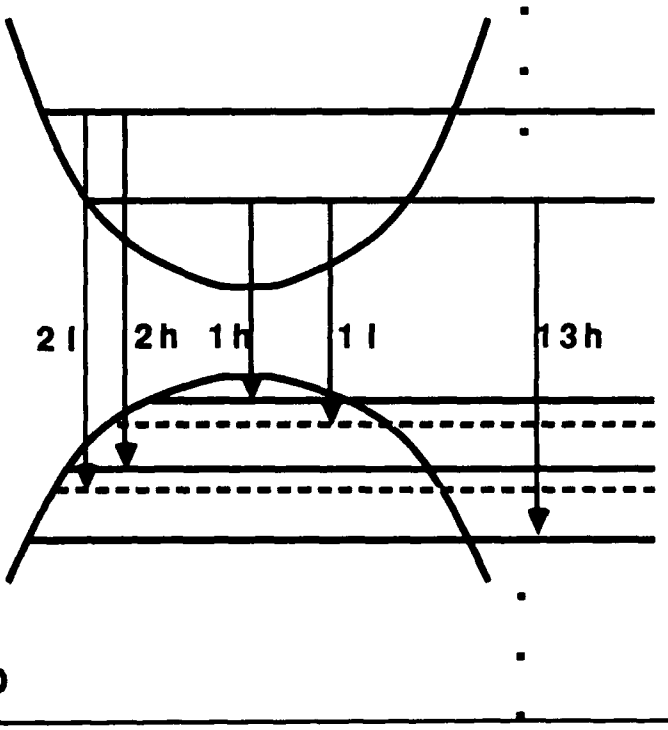

Fig. 5

PHOTOLUMINESCENCE DATA

Photoluminescence excitation (PLE) spectrum of parabolic quantum well reflecting harmonic-oscillator like transitions between electron and heavy-hole states.

Well width = 520Å; x=0 at well centre to x=0.3 at well edges.

Experimental and Calculated Energy-Level Spacings		
	Expt.	Calculated
electron	25.2 meV	27.6 meV
heavy-hole	10.5 meV	8.7 meV

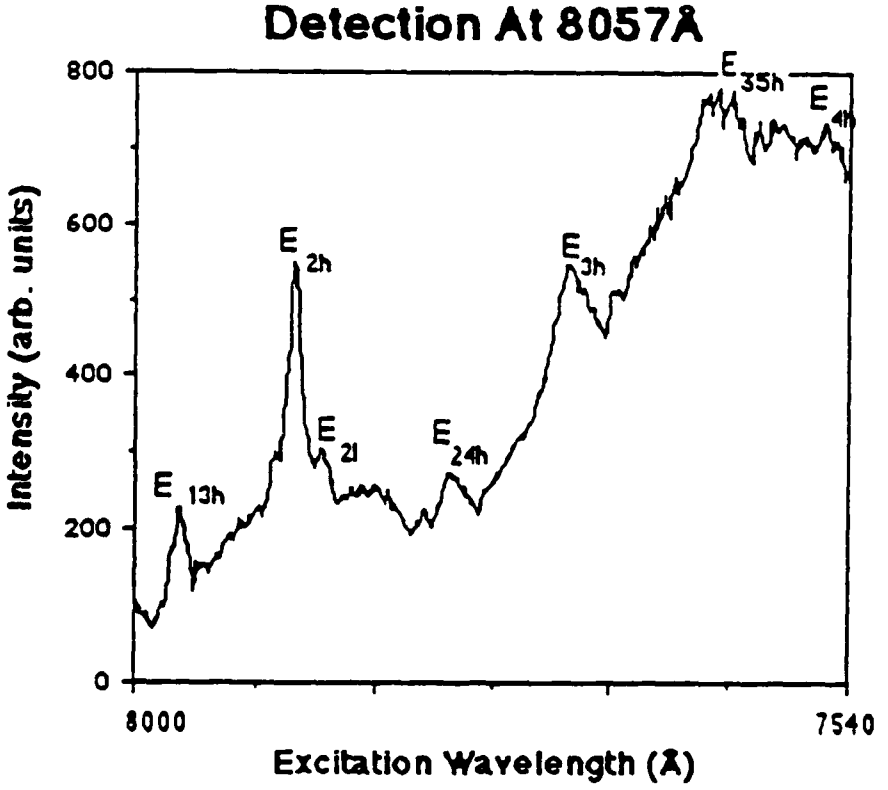

Fig. 6

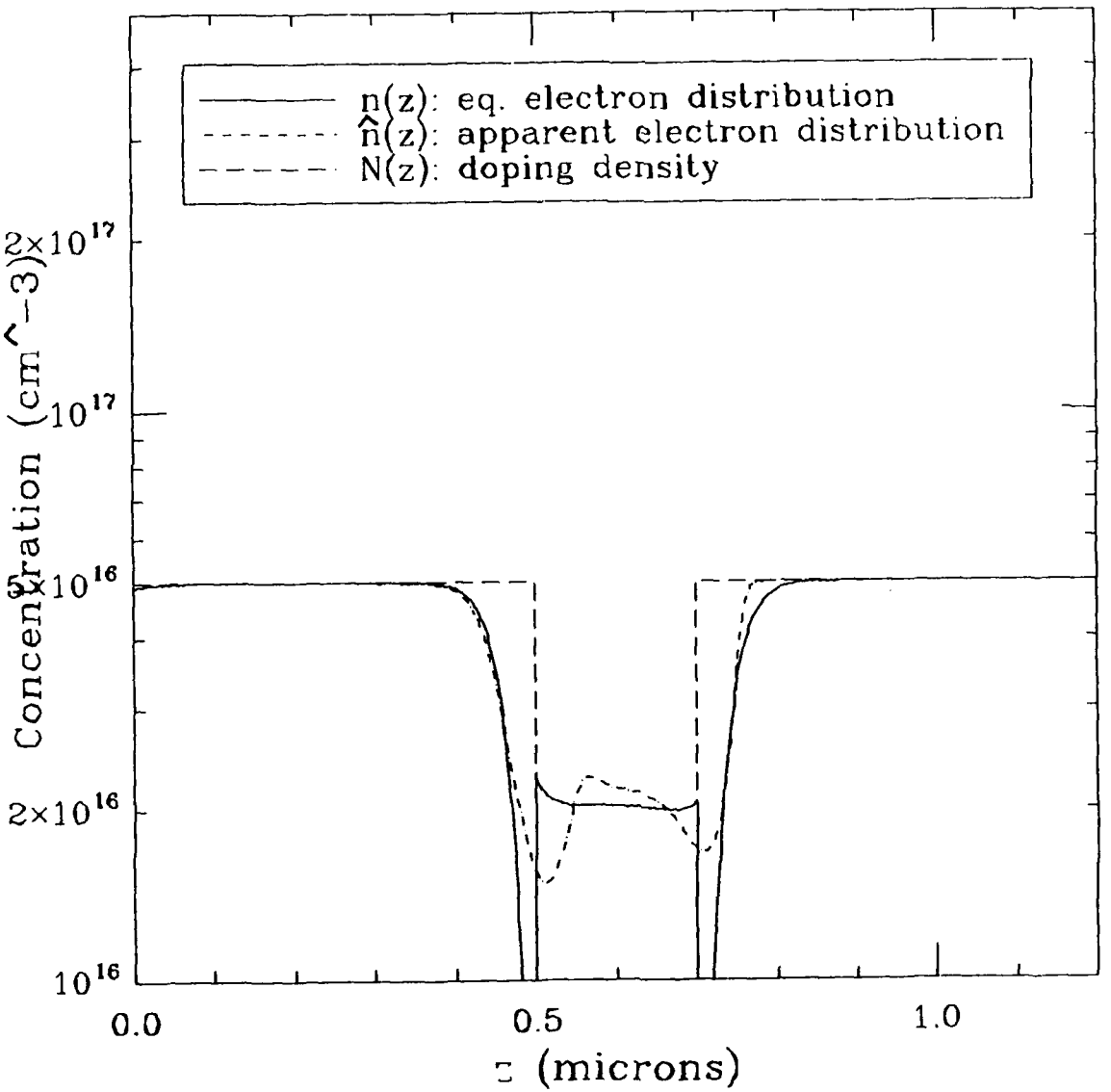
n(z): eq. electron distribution
n̂(z): apparent electron distribution
N(z): doping density
Concentration (cm^-3)
2×10^17
10^17
2×10^16
10^16
0.0
0.5
1.0
z (microns)

Fig. 7

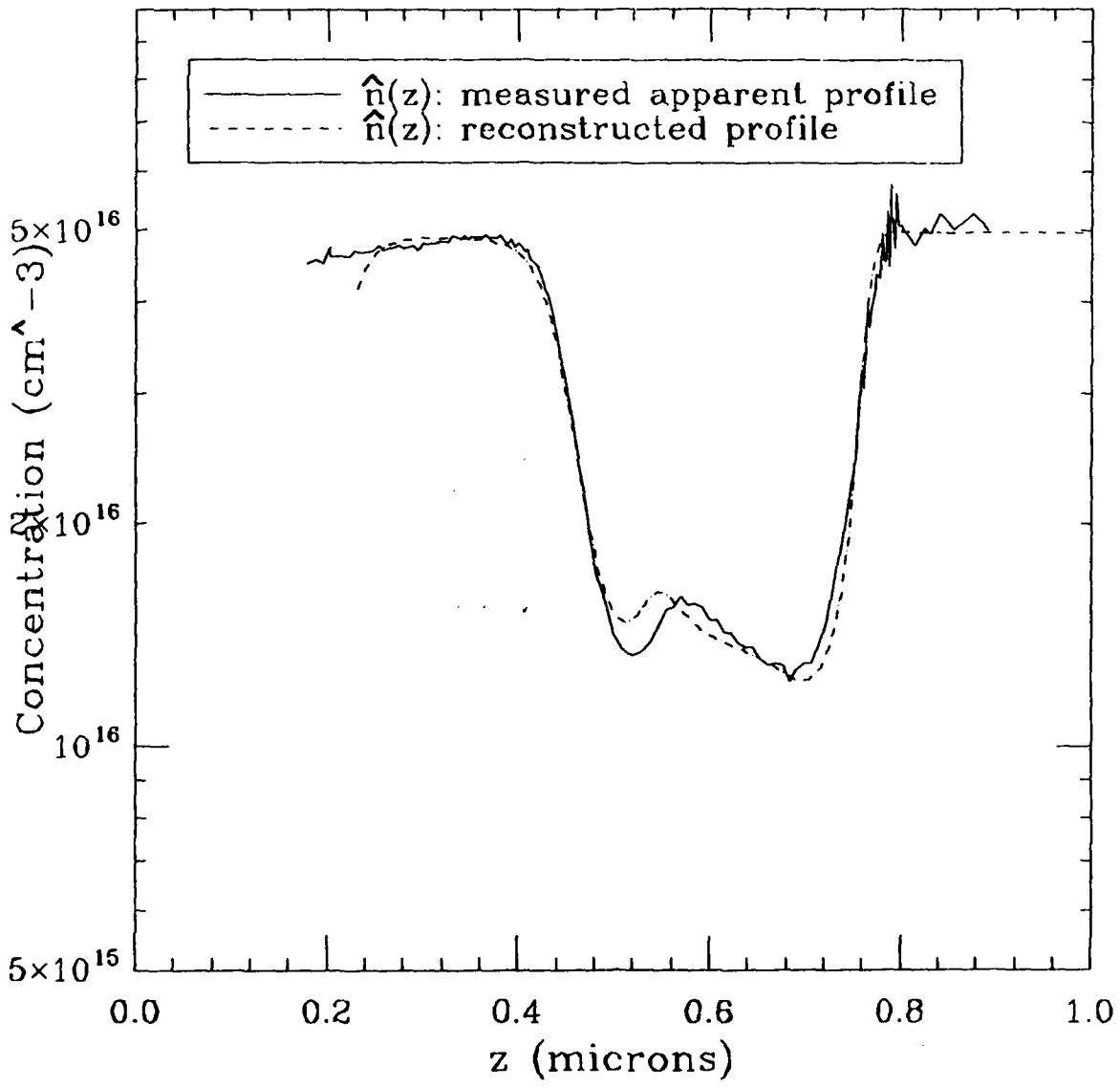
n̂(z): measured apparent profile
n̂(z): reconstructed profile
Concentration (cm^-3)
5×10^16
2×10^16
10^16
5×10^15
0.0
0.2
0.4
0.6
0.8
1.0
z (microns)

Fig. 8

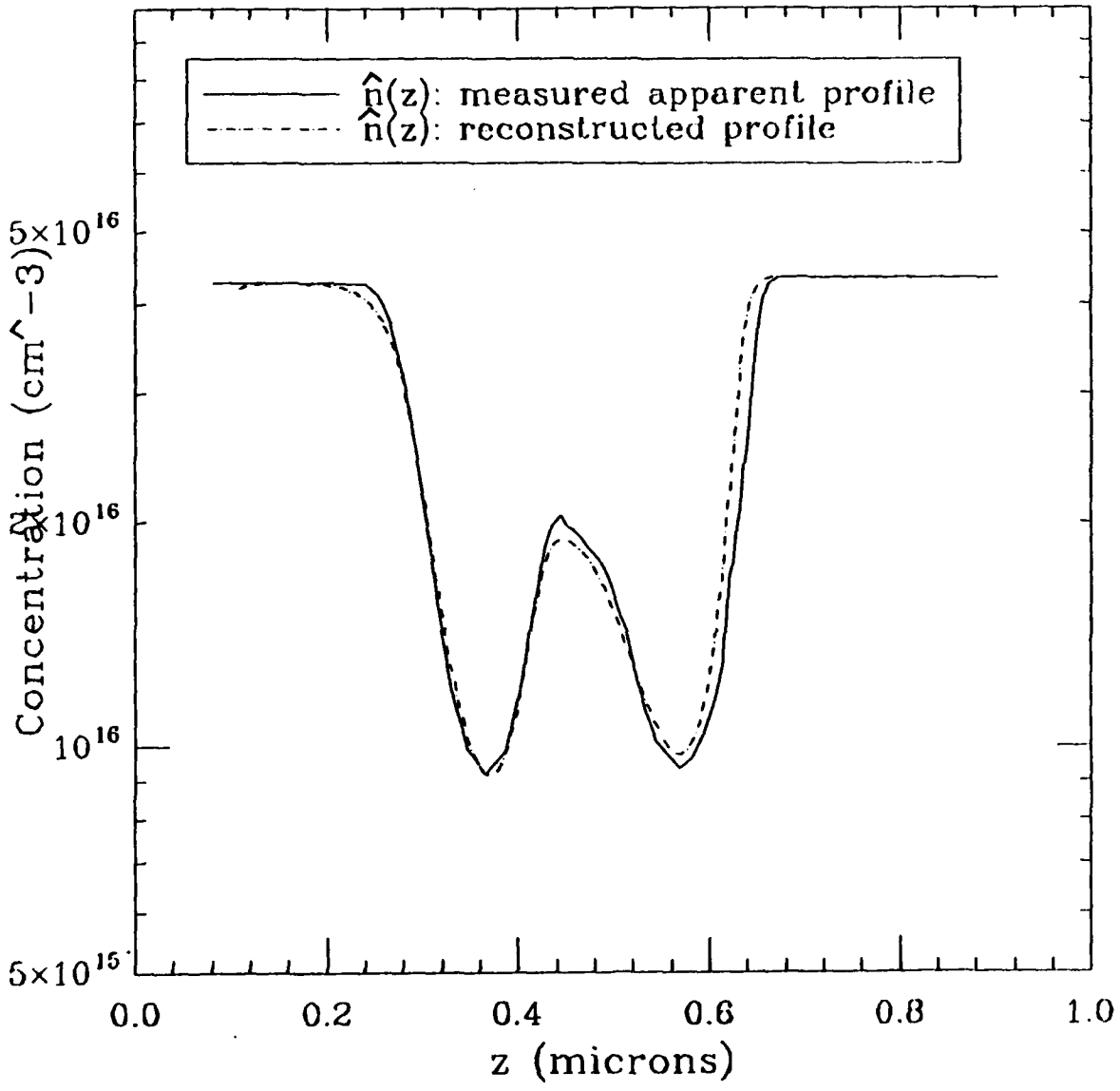
$\hat{n}(z)$: measured apparent profile
$\hat{n}(z)$: reconstructed profile
Concentration (cm^-3)
5×10^16
10^16
5×10^15
0.0
0.2
0.4
0.6
0.8
1.0
z (microns)

Fig. 9

conferences on high magnetic fields and on superlattices, microstructures and microdevices. A published report of the work will soon appear in Physical Review B, Rapid Communications in a paper entitled "Quantum Hall Effect in Wide Parabolic GaAs/AlGaAs Wells", by E. G. Gwinn, R. M. Westervelt, P. F. Hopkins, A. J. Rimberg, M. Sundaram, and A. C. Gossard. Manuscripts of this paper and the conference presentations are attached to this report. The structures exhibit both integral and fractional quantum Hall effect and show a transition from two toward three dimensional behavior as photoinduced carriers are added to the wells.

Future Plans:

In the next few months, we will exploit the added information now available from the capacitance and other characterization techniques to produce increasingly ideal structures for study of the high magnetic field ordering phenomena.

The parabolically graded structures may offer potentially interesting infrared behavior which is related to electron plasma motion in the parabolic potentials. Some of our initial thoughts in this direction are presented in a patent disclosure by Joe Maserjian, who visited Santa Barbara from the Jet Propulsion Laboratory during the year, and proposed a tuneable source of infrared radiation based on a modified parabolic structure. A copy of this disclosure, entitled "Tunable Submillimeter Wave Generator", is attached to this report.

We plan to make initial measurements of the infrared properties of the materials by means of Fourier transform infrared spectrometry, which is available to us through collaborations with the staff and students of the Quantum Institute, under Professor Jaccarino's direction here in Santa Barbara. An added possibility available to us through this channel is study of the structures in the intense tunable infrared beam of the Institute's free electron laser. We are initiating work in this direction through collaboration with newly arrived Assistant Professor Mark Sherwin, who will be making observations with the free electron laser on our materials and searching for nonlinear or chaotic responses in the infrared photoconductivity of the structures.

We will also hope to explore electrical transport in the third dimension and possible applications of the controlled electron density structures that we are building, to gated electronic devices.

Personnel:

The graduate student who has had major responsibility in all aspects of this research is Mr. Mani Sundaram. He is an outstanding third year student with excellent analytical and experimental skills who, among other honors, is a University of California Regents Fellow and topped his cadre in our PhD screening examination. Before starting the present research he had experience in Professor Steve Long's group in field effect transistor studies.

The newly arrived visiting researcher who will be working on this research is Dr. Achim Wixforth. He received his PhD degree one year ago at the University of Hamburg in the group of Professor Jorg Kotthaus and has just completed the first year of a six year junior faculty appointment at Hamburg in one of the best programs in Europe in low dimensional structures. He brings expertise in measurements, fabrication, and quantum physics to our effort.

Mr. John English, who worked with me at Bell Laboratories, is an important part of our research effort. He is supported as a Senior Development Engineer with hard money by the University of California. He has been extraordinarily valuable in setting up the laboratory and supervising its smooth operation and the growth of the materials.

REMOTELY-DOPED GRADED POTENTIAL WELL STRUCTURES

M. Sundaram, A. C. Gossard, and J. H. English
Dept. of Electrical and Computer Engineering, and Materials Dept.
University of California, Santa Barbara, CA 93106
(805) 961-8154
&
R. M. Westervelt
Division of Applied Sciences and Department of Physics
Harvard University, Cambridge, MA 02138

(Received: 15 April, 1988)

We present a new method to obtain high-mobility three-dimensional electron gas systems. We have achieved control of carrier density and of carrier profile by growth of the first remotely-doped parabolic potential well structures. Computer-controlled molecular beam epitaxy is used to grow a layer of ultra-fine superlattices with a programmable composition gradient. This produces conduction-band potentials which, in the absence of doping, are equivalent to the potential profiles of fixed charge distributions. When conduction electrons are introduced into these graded wells through remote doping of the barrier regions, they distribute themselves in such a way as to produce a uniform chemical potential at thermal equilibrium. We illustrate through computer simulations employing Fermi statistics that electrons introduced into a wide parabolic potential well distribute themselves uniformly. More significantly, the carrier distribution in the well is remarkably insensitive to the dopant sheet charge in the barrier, the more so at lower temperatures. We have fabricated remotely-doped graded potential well structures of the proposed type by molecular beam epitaxy. These structures exhibit the above effects. Measured mobilities of such three-dimensional electron gases grown using the GaAs/$Al_xGa_{1-x}As$ system are higher than those of bulk-doped GaAs doped to give the same uniform electron concentration.

1. INTRODUCTION

In this paper, we explore a means for producing high-mobility conduction electron gases of uniform and controlled density in semiconductors.

A useful construct in the theory of electrons in matter has been the concept of *jellium*: a neutral medium consisting of an electron gas moving in a uniform positively-charged background[1]. Such a hypothetical construction permits the calculation of the properties of a distributed electron gas without having to include the effects of the discretely charged ion cores of the host or dopant atoms in real solids. These calculations predict a number of interesting many-electron effects, many of which have not been observed experimentally, because of the difficulty of obtaining *jellium* in real solids[2].

For example, the ground state of a uniform electron gas in a semiconductor, at low temperature and in the presence of a strong magnetic field, is predicted to undergo a spin density wave transition to an ordered state with highly anisotropic conductivity[3]. But scattering from dopant ion cores and insulating transitions caused by electron binding to ion cores have thus far prevented observation of the predicted spin density wave state.

The experimental situation for the two-dimensional electron gas has been considerably better. The modulation-doped semiconductor heterostructure[4] and the metal-oxide-semiconductor transistor have provided two-dimensional electron gases confined at interfaces and moving with high mobility in channels containing no dopant ions. And, in these structures, the novel ordering phenomena of the quantum Hall effect[5] and the fractional

0749-6036/88/060683+09 $02.00/0

quantum Hall effect[6] have been observed. However, the charges on the barriers or gates and the electron gases in these structures introduce electric fields which have heretofore precluded more uniform electron distributions.

Pulse-doped semiconductors offer only minor improvement in the problems of electron scattering by dopant ions and low temperature carrier freeze-out that plague doped bulk semiconductors[7].

Thus, there has not been comparable progress in the production of high-quality three-dimensional electron gases.

The concept that we introduce here to achieve a uniform electron charge distribution without strongly-scattering ionic charge centers is a potential well with a graded composition profile and with conduction electrons introduced remotely from doped barrier layers. In the absence of conduction electrons, the conduction band-edge potential, $E_c(z)$, of the semiconductor is dependent on its composition, often varying linearly with composition. A graded composition profile leads to a graded band-edge profile.

The profile that is of particular interest to us is the parabolic potential profile inasmuch as such a profile exactly mimics the potential of a uniform positive quasi-charge distribution, ρ, where:

$$\frac{\partial^2 E_c(z)}{\partial z^2} = \frac{q\rho}{\varepsilon} \qquad (1)$$

Conduction electrons can then be introduced remotely into this graded region by doping barrier layers, having a higher conduction band edge, with donor atoms, whose electron charge transfers into the parabolic well. The charge transferred into the well will be distributed in such a way as to screen out the background potential and produce a constant electro-chemical potential in the structure at thermal equilibrium. If the width of the charge distribution is large enough that quantum confinement energies may be ignored, we recover the classical case of a uniform electron charge density, $\rho_e = -\rho$, throughout the region of the parabolic well occupied by the charge. We thus obtain the jellium approximation.

The dielectric permittivity, ε, in the equation above can be a function of distance z, through its dependence on the alloy composition of, say, the $GaAs/Al_xGa_{1-x}As$ system used to experimentally realize such a parabolic potential. It is seen from the above equation to be simply a parameter that relates the local carrier concentration to the local band curvature, and inasmuch as the relative dielectric permittivity changes fairly little from ~12.3 in the case of $Al_{0.3}Ga_{0.7}As$ to ~13.2 for GaAs, the deviations from the constant permittivity case, due to the resulting scaling, are small.

The graded-composition concept is entirely general and is applicable to more than the simple case of the parabolic potential considered in this paper. A conduction-band potential, in the absence of doping, exactly mimics the potential of the fixed quasi-charge background distribution that is proportional to its second derivative. If conduction electrons are introduced into such a potential through remote doping of the barrier regions, they would redistribute themselves in such a way as to screen out the background potential and produce a uniform electro-chemical potential at thermal equilibrium. This redistribution mechanism can be exploited to generate a large variety of carrier profiles.

The alloy-produced profile can be made much smoother than the spiked, strongly-scattering potential distributions of discrete dopant ions. As the carriers in the remotely-doped structure are isolated from the dopant ions the mobility of such an electron gas, even in the presence of alloy-disorder scattering, should be significantly higher than for a similarly doped bulk semiconductor.

2. SIMULATION RESULTS

To explore the wide parabolic well structure in some detail, consider Figs. 1. Fig. 1a shows the layer structure of the parabolic well with the doped barrier layers, and Fig. 1b the energy band diagram as it would look if there were no doping in the barrier layers, negligible residual background doping, and uniform dielectric permittivity and effective electron mass throughout the sample. The design parameters of interest are also depicted in Figs. 1, the being:

- a — half the width of the parabolic well
- b — the width of each doped barrier layer
- Δ_1 — the height of the parabola
- Δ_2 — the height of the barrier between the edge of the parabola and the doped barrier layer
- n_d — the barrier layer doping

In a first-order approximation, if we assume that a uniform electron concentration 'n' exists in the well at thermal equilibrium, we set the parabolic band bending resulting from this constant negative charge to cancel the parabolic band offset prevailing in the original structure as:

$$\frac{q\,n\,a^2}{2\varepsilon} = \Delta_1\,(eV)$$

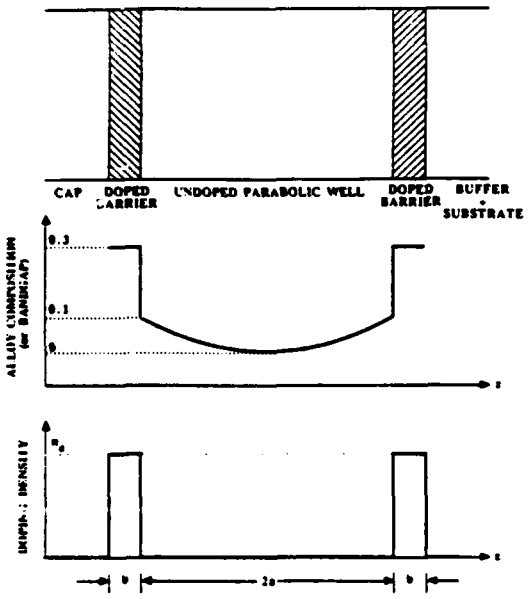

Fig. 1a. Layer structure, alloy composition and doping distribution of the wide symmetric-parabolic well. The barriers are doped to a width b at a concentration n_d.

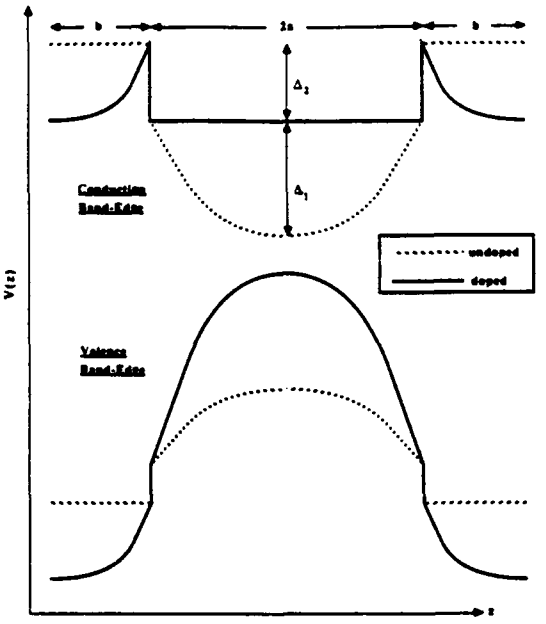

Fig. 1b. Energy-band diagram (not drawn to scale) for the layer configuration shown in Fig. 1a. Bold lines show energy-band diagram at thermal equilibrium with the barrier layers doped to give flat-band conditions in the well. Dotted lines depict the design parabola energy bands (obtained by computer-controlled MBE), assuming no doping, uniform dielectric permittivity and uniform effective electron mass through the layers. Δ_1 is the depth of the conduction-band parabola, Δ_2 the barrier between the edges of the conduction-band parabola and the barrier layers. The width of the graded layer is 2a.

Taking, for instance, $n = 1.25 \times 10^{16}$ cm^{-3} and $\Delta_1 = 0.081$eV, gives: a ~ 1000Å. Besides, charge neutrality requires that:

$$n\,a = n_d\,b \qquad (3)$$

A doping of $n_d = 6.25 \times 10^{17}$ cm^{-3} gives: b = 20Å.

With these design parameters, we expect near flat-conduction-band conditions to prevail in the well at thermal equilibrium. A computer simulation that assumes a certain center-well concentration and on the basis of that assumption, calculates the charge, field and potential distributions, till the condition of charge neutrality is satisfied in the structure, is expected to converge in such a flat-band state. The sheet charge in each barrier layer, $n_d b$, appears the most critical parameter affecting this ideal case, and it would be instructive to study the effect of its variation on the equilibrium band profile and well electron distribution.

To this end, the well is divided into a number of sufficiently small cells. One guesses a center-well electron concentration, which pins the Fermi level with respect to the conduction band at the center of the well. The electron concentration in the next cell is iteratively obtained from the Joyce-Dixon approximation. The field and potential drops across this cell are then obtained from Poisson's equation and added to the local band bending (i.e. the design parabola) to get the new band shape in the cell. The process is repeated for successive cells through the end of the doped barrier, where the field is monitored. Zero field at this point indicates convergence. A positive or negative field implies that our initial guess was too high or too low. A corrected guess at the center-well concentration is then made and the above sequence of calculations carried through. Using bisection, convergence is fairly rapid. A 3D parabolic density of states is assumed for the conduction band.

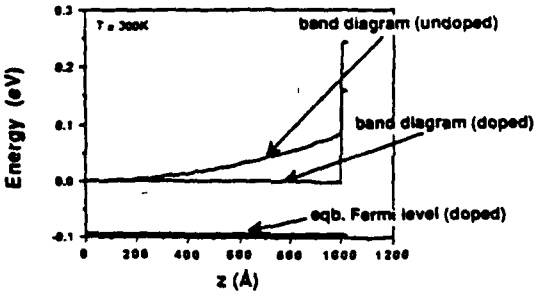

Fig. 2a. Thermal equilibrium conduction-energy-band diagram and equilibrium fermi level for the right half of the symmetric parabolic well and for a set of parameters designed to give flat-band conditions and uniform electron distribution in the well at 300K: Δ_1=0.081eV, n_d=6.25x10^{17} cm^{-3}, a=1000Å, b=20Å, giving n = 1.2x10^{16} cm^{-3}. The design parabola is also shown for reference.

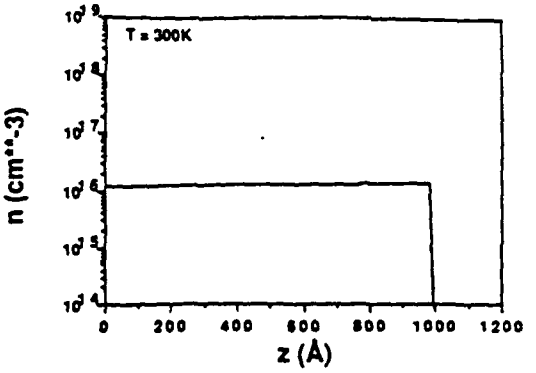

Fig. 2b. Electron distribution in the parabolic well at thermal equilibrium for the design parameters used to get the energy-band configuration in Fig. 2a. Temperature = 300K.

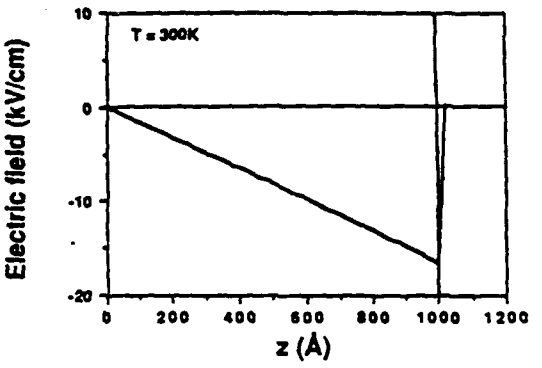

Fig. 2c. Electric field distribution for the right dipole created by the sheet of positive donor ions in the barrier layer and the plasma of uniformly distributed electrons in the well. Field goes to zero at dipole boundaries as expected by Gauss' law. An exactly symmetric but opposite dipole exists in the left half of the well.

The variation of both the dielectric permittivity, $\varepsilon(z)$, and the electron effective mass, $m^*(z)$, (as it occurs in the conduction band effective density of states, $N_c(z)$, that is used in the 1-D approximation) in the well are easily included in the above analysis. As stated previously, the dielectric permittivity is simply a scaling factor. The local electron concentration, n(z), is directly proportional to the local $N_c(z)$, which in turn is proportional to $(m^*(z))^{1.5}$. For the GaAs/$Al_xGa_{1-x}As$ system, m^* varies, approximately linearly, from ~ 0.07m_e for GaAs to ~ 0.09m_e for $Al_{0.3}Ga_{0.7}As$ (here m_e is the free electron mass). This translates to a 50% maximum change in the electron concentration from the constant m^* case. The results presented in the current study assume constant ε and m^*.

The results of a simple classical analysis, assuming a temperature of 300K, are shown in Figs. 2. For a particular set of design parameters, Figs. 2a, 2b and 2c show the band diagrams and equilibrium Fermi level, the electron distribution and the electric field distribution, respectively. The symmetry of the structure under analysis permits us to graph these values for just one half of the structure. In Figure 2a, we use the term *band diagram (undoped)* to denote the case where there is no doping in the barrier layers and where the conduction band is consequently the design parabola. Fig. 2a shows the initial and equilibrium band diagrams and the equilibrium Fermi level. The doping and thickness of the barrier layer (in other words, the sheet barrier charge) were chosen as per the above analysis to give flat-band conditions and a uniform electron concentration in the well at equilibrium. These are seen to be indeed the case from Figs. 2a and 2b. The electric field in Fig. 2c satisfies Gauss' law, going to zero at the boundaries, indicating net zero charge in the structure; the equal positive and negative charges provided by the doping are simply redistributed, the positive donor ions remaining immobile in the barrier layers and the electrons arranging themselves in the manner shown in Fig. 2b.

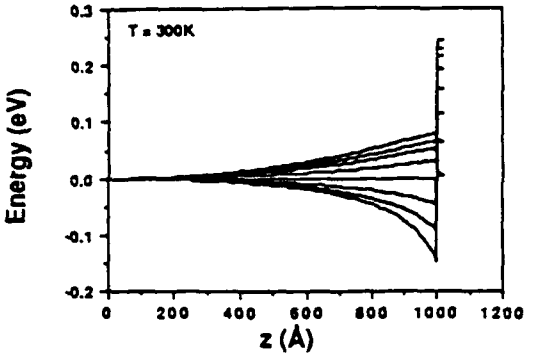

Fig. 3a. 300K thermal equilibrium energy-band diagrams for the right half of the symmetric parabola for a range of barrier dopings from $n_d/8$ to $8*n_d$, for the same set of design parameters used in Fig. 2a. The lowermost curve corresponds to $8*n_d$, with doping decreasing for each upper curve by a factor of 2 down to $n_d/8$. The topmost curve is the design parabola.

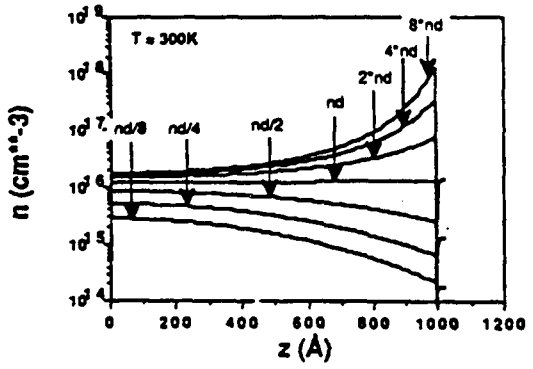

Fig. 3b. 300K thermal equilibrium electron distributions in the right half of the parabolic well corresponding to the energy-bands in Fig. 3a.The barrier dopings are indicated in the figure. The electron distribution remains approximately constant over most of the well for the range of barrier dopings indicated, the excess or deficit being inserted in or extracted from the edges.

Figs. 3 thru 5 show the thermal-equilibrium energy-band diagrams and electron distributions at three different temperatures (300K, 77K, 0K), for the above set of design parameters, with the barrier doping concentration as a parameter that is varied within each set. In each of these figures, n_d refers to the value calculated to give flat band conditions at equilibrium. The doping is varied from $n_d/8$ to $8*n_d$.

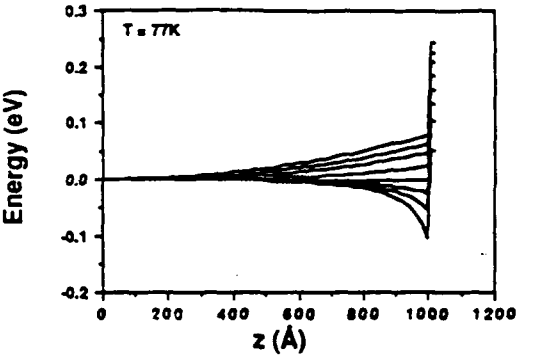

Fig. 4a. 77K thermal equilibrium energy band diagrams for the same set of design parameters and the same range of barrier dopings used in Fig. 3.

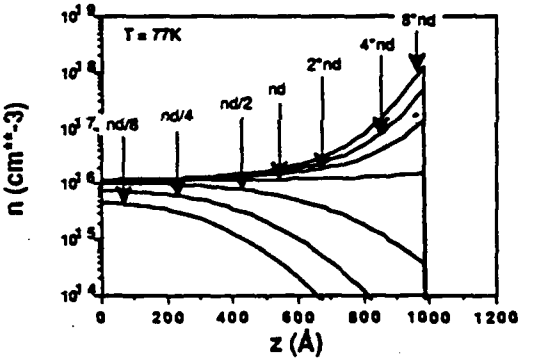

Fig. 4b. Electron distributions in the well at 77K corresponding to the different energy bands in Fig. 4a.

The main point to emerge from these figures is that the electron concentration over most of the parabolic well remains almost constant over the range of doping shown. At doping concentrations below n_d, the electrons are lost more from the edges of the well than from the center where they are held approximately to their values at doping n_d. At doping concentrations above n_d, the extra electrons start accumulating toward the edges, their values over most of the well width again fairly constant at their values at

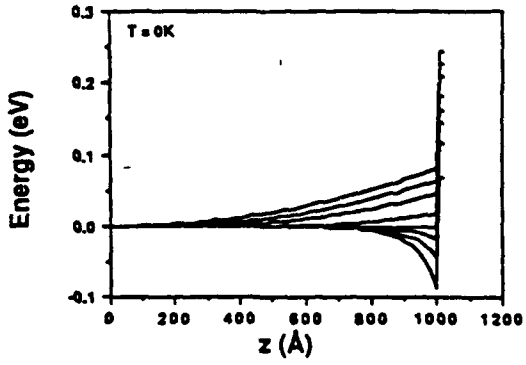

Fig. 5a. Thermal equilibrium energy band diagrams for the parabolic well at a temperature of 0K for different barrier dopings and the same set of design parameters used in Figs. 3 and 4.

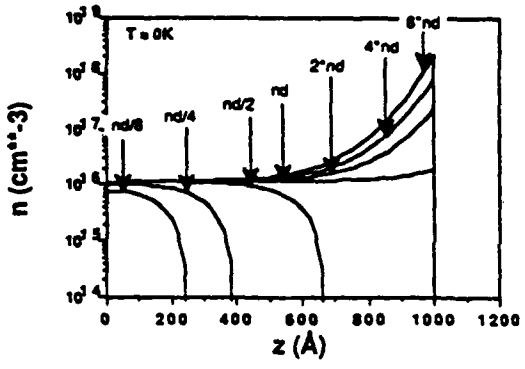

Fig. 5b. Electron distributions in the well at 0K corresponding to the different energy bands in Fig. 5a.

doping n_d. This suggests that, in these doping ranges, the electron concentration over most of the well is determined by the curvature of the design parabola.

These trends are evident in the structure at all three temperatures, the approach to the ideal classical case increasing with decreasing temperature.

The maximum thickness, L_{max}, of the uniform electron gas that can be obtained by the graded potential well technique described here is determined by the desired charge density, ρ_e, of the electron gas, the available barrier height, and the lowest donor energy level in the doped barrier (measured from the bottom of the parabolic potential well), V_D, as per:

$$L_{max} = 2\sqrt{\frac{2V_D\varepsilon}{\rho_e}} \qquad (4)$$

The maximum V_D is $\Delta_1 + \Delta_2$, if the donor binding energy in the doped barrier is ~0 and the doping so high that the band-bending in the barrier is much less than Δ_2.

In the undoped design parabolic potential well, the analysis for which was presented above, the spacing between the energy-eigen values in the well is approximately constant at 4 meV. When the doping is smaller than the value required to give flat-band conditions in the well, the well is flattened, but still approximately parabolic in shape, the energy level spacing consequently reducing by a factor ~ $(\Delta/\Delta_1)^{1/2}$, where Δ_1 is the original height of the undoped design parabolic potential well, and Δ the reduced height. When flat-band conditions are reached, we have, of course, the case of a wide square potential well of height Δ_2, the barrier height, and for the above design parameters the energy levels measured from the well bottom go approximately as n^2E_0, where E_0 ~ 0.14 meV and n = 1, 2, ... are the various levels. For higher doping, most of the well is flat and the above energy levels for the flat-band case still hold. The accumulation of electrons at the well-edges with increasing barrier doping results in potential notches at the edges which perturbs these energy values. The energy in the notches is certainly quantized for high doping and in the case where these notches are at their narrowest (for the high doping $8*n_d$ at 0K - refer to Fig. 5a), the energy levels for the above design parameters are approximately 0.12 eV, 0.22 eV, ... A_nE_0, (measured from the bottom o the notch), where A_n is the n-th root of the Airy functior and E_0 ~ 52.7 meV.

3. EXPERIMENTAL RESULTS

The materials system that we have used in an attemp to realize the approximation experimentally is a GaAs $Al_xGa_{1-x}As$ heterostructure configuration containing graded superlattice and silicon-doped barrier layers. Bar gap energies and electron affinities in these alloys a functions of alloy composition. Precision control ar grading of the alloy composition is possible throug computer-controlled molecular beam epitaxy. Using th principle, undoped parabolic quantum wells have be grown before[8] and the well profile characterized throu optical studies. The individual layers of the grad

Parameter	Value
Δ_1	0.081eV
Δ_2	0.155eV
2a	2000Å
b	100Å
n_d	$2.0\times10^{17}cm^{-3}$
setback	200Å
$X_{Al\_well\text{-}centre}$	0
$X_{Al\_well\text{-}edge}$	0.1
$X_{Al\_barrier}$	0.3

Table 1. Structural parameters of sample 1, Van der Pauw measurements for which are presented in this paper. (*See text*).

superlattice are sufficiently thin that electrons readily tunnel through them, making 3D transport normal to the superlattice layers possible in the wells considered in this paper.

In the present study, a number of structures were grown in which a parabolically graded Al composition profile was approximated by a constant-period superlattice in which the relative thicknesses of GaAs and $Al_{0.3}Ga_{0.7}As$ in each superlattice period were incremented to yield an average composition that matched the desired parabolic profile. A semi-insulating (100)-oriented GaAs substrate at a temperature of 600 °C was used for the growth, which took place under arsenic-rich growth conditions under a continuous flux of As_4 from a solid As source. The structural parameters of a sample (referred to henceforth as sample 1) with a 2000Å wide parabolic well for which measurements are presented in this paper are shown in Table 1. The chopping period used was 20Å, which, for an Al composition varying parabolically from 0% at the well-center to 10% at the well-edges implies that the duty-cycle L_z of the $Al_{0.3}Ga_{0.7}As$ in each period, as a function of distance z from the center of the well, is given by:

$$L_z = 20\,\text{Å}\,(\tfrac{1}{3})(\frac{z}{1000\,\text{Å}})^2 \qquad (5)$$

Van der Pauw measurements on this sample at a temperature of 77K yielded a sheet carrier concentration $n_s = 3.7\times10^{11}$ electrons/cm^2 and an electron mobility (parallel to the superlattice layers) μ_e = 27,000 cm^2/Vs. (Room temperature values were 3.9×10^{11} electrons/cm^2 and 5900 cm^2/Vs.) In the presence of the potential curvature from the aluminum composition gradient, these electrons should be distributed nearly uniformly to occupy most of the potential well. The curvature of this parabolic well corresponds to a constant positive quasi-charge density of $\sim 1.2\times10^{16}$ cm^{-3}, implying a constant electron concentration of the same value, on doping the barriers. Occupation of the well by the observed low-temperature sheet charge density of 3.7×10^{11} cm^{-2} then implies that 50% more than the number of electrons required to give a

Parameter	Value
Δ_1	0.155eV
Δ_2	0.143eV
2a	2000Å
b	100Å
n_d	$2.1\times10^{17}cm^{-3}$
setback	200Å
$X_{Al\_well\text{-}centre}$	0
$X_{Al\_well\text{-}edge}$	0.2
$X_{Al\_barrier}$	0.4

Table 2. Structural parameters of sample 2, Hall measurements for which are presented in this paper. (*See text*).

uniform carrier distribution in the well, has been deposited in it. Our simulation results suggest that the excess electrons would be mostly inserted near the well-edges, whereas over most of the well width the concentration would be held approximately near the value determined by the curvature of the design parabola, viz. 1.2×10^{16} cm^{-3}. The electrons near the well-edges will scatter more strongly from the ionized impurities in the barriers, reducing the overall mobility of the 3D plasma. A larger setback and a more uniform electron distribution in the well (through a smaller doping) should significantly enhance this mobility.

A Hall measurement (dark) on another part of sample 1 yielded a 1.6K mobility μ_e = 19,000 cm^2/Vs at a sheet concentration $n_s = 2.0\times10^{11}$ cm^{-2}. This decrease in mobility and sheet concentration from 77K suggests the presence of a highly-scattering ionized-impurity concentration in the well in this sample. Optimized growth conditions should enhance the low temperature mobility.

From the measured n_s value at 1.6K above, we deduce that the 4 lowest energy subbands in this 2000Å-wide square well are occupied, at this temperature. It i interesting to note that given the width of the well and th consequent closeness of the energy-eigen values, th electron concentration calculated from the approximate 3I parabolic density of states for the conduction band, is onl about 20% larger than if calculated from the 2D density c states, at this temperature.

In sample 2, the design parameters for which ar listed in Table 2, fewer than the number of electror required to fill the well were deposited. The width of th parabolic well is the same as for sample 1, viz. 2000Å, b the Al composition increases parabolically from 0% at th well-center to 20% at the well-edges, implying twice t curvature of the first parabola and corresponding therefc to a uniform electron density of ~ 2.3×10^{16} cm^{-3} thermal equilibrium in the well. The 4.2K Hall mobilit (parallel to the superlattice layers) measured on this samp were 200,000 cm^2/Vs (dark and light). The occupation the well at this temperature by the measured electron sh concentration of 2.1×10^{11} cm^{-2} then implies that abc 930Å of the central portion of the well is filled (a

uniform density of ~ 2.3×10^{16} cm^{-3}), the result of providing only about half the number of electrons required to completely fill the well at the uniform concentration determined by the parabola curvature. The 300K and 77K mobilities of the electron gas in this sample were respectively 3900 cm^2/Vs and 56,000 cm^2/Vs, the corresponding measured electron sheet concentrations being 5.38×10^{11} cm^{-2} and 2.58×10^{11} cm^{-2}. The fact that the electrons are bunched together about the well-center, away from the doped barriers, will of course significantly enhance their mobility.

The equilibrium conduction-band in this case will be approximately still a parabola, shallower than the design parabola by a factor of ~ 2. One then deduces from the n_s measured at 4.2K above that the 2 lowest subbands of this parabolic well are occupied at this temperature.

4. CONCLUSION

In conclusion, we have proposed a novel method to obtain high-mobility three-dimensional electron gas systems. This method, featuring precision control over the carrier density and over the carrier profile, involves the growth of compositionally-graded, remotely-doped potential well structures.

Computer-controlled MBE is used to grow ultra-fine superlattices with a programmable composition gradient. This produces conduction-band potentials which, in the absence of doping, replicate the potential profiles expected of fixed quasi-charge background distributions. Conduction electrons introduced into the graded wells through remote doping of the barrier regions, distribute themselves in such a way as to screen out the background potential and produce a uniform electro-chemical potential at thermal equilibrium. This redistribution mechanism can be exploited to generate a large variety of carrier profiles.

We have studied the case of the graded parabolic potential and have shown through simulations employing Fermi statistics, that in this particular case, the electrons introduced through remote doping indeed distribute themselves uniformly over the well width, the concentration value being determined almost exclusively by the curvature of the parabolic well. Our simulations also show that this constant distribution is remarkably tolerant of doping variations, the more so at lower temperatures.

We have grown and measured the mobilities of such structures. The 77K mobility values are higher than or comparable to the mobilities at any temperature of similarly bulk-doped GaAs (typically 15,000 cm^2/Vs at 77K for 1-2 $\times 10^{16}$ cm^{-3} doping), illustrating the effect of the reduced ionized-impurity scattering that the electrons would benefit from, given their isolation from the dopant ions.

ACKNOWLEDGEMENTS- We thank Hörst Störmer and Joe Maserjian for discussions, and P. O. Holtz for discussions and photoluminescence measurements on the undoped parabolic quantum wells. We thank Bert Halperin for discussions and for pointing out the carrier density dependence on the potential curvature, and Beth Gwinn for electrical measurements. Sample 2 was grown at AT&T Bell Labs. We acknowledge Kirk Baldwin for the mobility measurements on this sample. This work was supported in part by the U.S. Air-Force Office of Scientific Research under contract # AFOSR-88-0099.

References

1. David Pines, Elementary Excitations in Solids, New York, W. A. Benjamin (1963), Series Title: Lecture Notes and Supplements in Physics 5.
2. V. Celli and N. David Mermin, Physical Review **140**, Number 3A, A839 (1965).
3. B. I. Halperin, Proceedings of the 18th International Conference on Low Temperature Physics, Kyoto, 1987; (Japanese Journal of Applied Physics **26**, Suppl. 26-3, Part 3 (1987)).
4. R. Dingle, H. L. Störmer, A. C. Gossard, and W. Wiegmann, Applied Physics Letters **33**, 655 (1978).
5. K. von Klitzing, G. Dorda, and M. Pepper, Physical Review Letters **45**, 494 (1980).
6. D. C. Tsui, H. L. Störmer, and A. C. Gossard, Physical Review Letters **48**, 1559 (1982).
7. K. Ploog, Journal of Crystal Growth **81**, 304 (1987).
8. R. C. Miller, A. C. Gossard, D. A. Kleinman, and O. Munteanu, Physical Review B, Condensed Matter, **29**, Number 6, 3740 (1984).

Proc. 4th Int. Conf. on Superlattices, Microstructures and Microdevices, Trieste, 1988
to appear in Superlattices and Microstructures

QUANTUM HALL EFFECT IN WIDE PARABOLIC GaAs/$Al_xGa_{1-x}As$ WELLS

E.G. Gwinn, R.M. Westervelt, P.F. Hopkins, and A.J. Rimberg
Division of Applied Sciences and Department of Physics
Harvard University, Cambridge MA, 02138

M. Sundaram and A.C. Gossard
Department of Electrical and Materials Engineering and Materials Department
University of California, Santa Barbara CA, 93106

(Received 8 August, 1988)

Parabolic well structures have been proposed to produce thick spatially uniform regions of dense high mobility electron gas. Wide parabolic GaAs/$Al_xGa_{1-x}As$ wells were fabricated using molecular beam epitaxy by grading the average Al concentration. These structures have high mobility at low temperatures ($\mu = 5x10^4$ to $2.5x10^5$ $cm^2/Vsec$) and show the integer and fractional quantum Hall effect. Characteristic changes in the integer quantum Hall effect and the longitudinal magnetoresistance in a 4000Å wide well are measured as the well is partially filled with electrons using persistent photoconductivity. These data establish that up to three electric subbands of the well are occupied.

The ability to produce narrow two-dimensional (2D) layers of high mobility electron gas in semiconductor structures has permitted the study of the 2D electron gas in strong magnetic fields under nearly ideal conditions, and led to the discovery of the integer and fractional quantum Hall effects[1]. The existence and form of the quantum Hall effect in three dimensional samples, as well as possible collective phenomena induced by strong magnetic fields[2], are topics of considerable interest. However, despite many interesting experiments, limited progress has been made for the three dimensional (3D) electron gas in semiconductors, due in part to the strong influence of the potential from dopant atoms. Notably, Störmer et. al.[3] observed the integer quantum Hall effect in a stack of weakly coupled electron sheets in a layered $GaAs/Al_xGa_{1-x}As$ heterostructure.

Remotely-doped parabolic $GaAs/Al_xGa_{1-x}As$ wells can be used to produce relatively thick layers of high mobility electron gas which are spatially uniform due to the action of the parabolic potential[2,4]. Very recently the 2D integer[5,6] and fractional[5] quantum Hall effect (QHE) has been measured in these structures in the high field regime for which only one electric subband is occupied. We report here measurements of the integer quantum Hall effect and longitudinal magnetoresistance R_{zz} for a thick (>1000 Å) electron layer in a parabolic $GaAs/Al_xGa_{1-x}As$ well. Persistent photoconductivity was used to study both the QHE and longitudinal magnetoresistance as the well was filled with electrons. These data show that filling of the well occurs at essentially constant Fermi energy while the subband energy decreases due to increased width of the electron layer, and show that more than one subband is occupied for the integer quantum Hall effect.

Figure 1 is a schematic illustration of the conduction band edge vs. position for empty and partially-filled parabolic wells[4]. For the empty well in Fig. 1a, the parabolic potential of depth Δ_1 is confined by a barrier of height Δ_2. Remotely located dopant layers in the barrier are used to fill the well with electrons. The essential idea needed to understand the filling of the well is that the parabolic potential is identical to that produced by a spatially-uniform positively charged background of 3D density $n_+ = 2\varepsilon\Delta_1/\pi e^2 w^2$. The electrons act to screen this fictitious positive charge as they enter the well. When the well is full, the electron density n is constant and equal to the design density n_+ over the entire width of the well, and the total potential is simply that of a square well of width w and depth Δ_2 in the Thomas-Fermi approximation. Even when the well is partially full, as in Fig. 1b, the electrons act to screen the parabolic potential and create a thinner slab of comparable density $n \cong n_+$ over part of the width w_e as indicated. For this case the total potential approximates that of a square well of width w_e. As the well is filled with electrons, the width w_e of the electron layer increases while the density n remains approximately constant. Thus this process is self correcting and does not require precise control of the doping to generate

spatially-uniform electron density profiles. These concepts are general, and can be used to create density profiles other than those in Fig. 1.

When a relatively small number of electric subbands of the well are occupied, as for the data discussed below, the discrete spectrum of electron energy levels in the well becomes important. To a first approximation, this is the energy spectrum $E_n = n^2(h/w_e)^2/8m_e$ of a square well of width equal to the thickness w_e of the electron layer. As the well fills with electrons and the electron layer becomes wider, the separation of these levels decreases as $1/w_e^2$. If more than one subband is occupied, the Fermi energy E_F changes relatively little as the well is filled, as for the 3D limit. Thus the number of occupied subbands increases while the Fermi energy remains approximately constant.

Parabolic well heterostructures were grown[4] using molecular beam epitaxy on semi-insulating GaAs substrates. The parabolic potential was created by changing the relative thickness of alternating GaAs and $Al_{0.3}Ga_{0.7}As$ layers in a fine superlattice of period 20 Å, with a $Al_{0.3}Ga_{0.7}As$ barrier. Electrons were deposited in the well from Si-doped layers in the barrier symmetrically set back from both sides of the well. Five structures have been grown and characterized to date with low temperature mobility as large as $\mu_H = 2.5 \times 10^5$ cm^2/Vsec. For the structure discussed here the well parameters are: width $w = 4000$ Å, parabolic well depth $\Delta_1 = 150$ meV (for which $n_+w = 2.2 \times 10^{11}$ cm^{-2}), and barrier height $\Delta_2 = 75$ meV.

Parabolic well samples were prepared in a Hall bar geometry defined using optical lithography. Electrical contacts were made by applying small amounts of In to the contact pads and baking at 400 C for ~ 5 min in a reducing atmosphere. The samples were mounted stress-free and cooled in the dark to $T = 50$ mK in a He dilution refridgerator. Magnetic fields to $H \sim 7$ Tesla were applied using a superconducting solenoid, and the Hall resistance, and the transverse and longitudinal magnetoresistance were measured using lock-in techniques. Typical values of the applied current were ~ 20 nA. Low field Hall effect measurements were used to determine the mobility $\mu_H = 4.4 \times 10^4$ cm^2/Vsec and the areal electron density $n_H = 0.78 \times 10^{11}$ cm^{-2} at low temperatures before illumination. These measurements indicate that the well is partially full as grown with $n_H/n_+w = 0.36$. Additional electrons were introduced into the well using persistent photoconductivity by illuminating the sample *in situ* with a light-emitting diode.

Figure 2 presents plots of the transverse magnetoresistance R_{xx} and the Hall resistance R_{xy} before (Fig. 2a) and after (Fig. 2b) a period of illumination. Hall data at low magnetic fields $H < 1$ Tesla determine the areal density, which increases substantially after illumination to $n_H = 1.12 \times 10^{11}$ cm^{-2}. However, the position and period of Shubnikov de Haas oscillations in the magnetoresistance remain practically unchanged, as shown in Fig. 2. Thus the cross sectional area of the Fermi

surface perpendicular to the field remains essentially constant, unlike the 2D case. In addition, the low field Shubnikov de Haas oscillations are not simply periodic after illumination. From the fast oscillation period in 1/H for Figs. 2a and 2b, we obtain the Fermi energy $E_F = 2.8$ meV of the electron gas in the well relative to the bottom of the lowest subband. The fact that the Shubnikov de Haas oscillations do not change as the areal density increases is direct evidence that more than one subband is occupied; for a 2D sample the oscillation period and Fermi energy both increase linearly with areal density. Longitudinal magnetoresistance measurements discussed below indicate that two subbands are occupied as grown, increasing to three following a period of illumination comparable to that for Fig. 2b.

A well defined integer quantum Hall effect is observed at higher fields both before and after illumination as shown in Figs. 2a and 2b for data taken at T = 50 mK. Broad flat steps in the Hall resistance $R_{xy} = (1/\nu)h/e^2$ are observed at integer values of the filling factor ν, which determines the number of spin split Landau levels below the Fermi energy. The magnetoresistance vanishes $R_{xx} \rightarrow 0$ at magnetic fields corresponding to Hall steps both before and after illumination. The small values of R_{xx} at Hall steps are evidence that electrons responsible for the Hall and magnetoresistance data in Fig. 2 are located in the well rather than in possible parallel conduction paths created by illumination.

It is interesting to consider the effect of increased areal density on the quantum Hall effect. As shown in Figs. 2a and 2b, both the Hall and magnetoresistance decrease with illumination as expected for a greater number of carriers. However, the position in magnetic field of the steps remains relatively unchanged at lower fields with increasing areal electron concentration, unlike the 2D case. For example, the location of the $\nu = 4$ step in Fig. 2a remains at the same field after illumination in Fig. 2b, as the filling factor increases to $\nu = 6$, indicating the addition of one Landau level below E_F. We interpret this increase in ν as the lowest Landau level of the second subband crossing below the Fermi energy at H = 0.8 Tesla. With increasing illumination the $\nu = 2$ step in Fig. 2a decreases in width and a $\nu = 3$ step appears and grows in width until the $\nu = 2$ step disappears entirely as in Fig. 2b. For a further increase in illumination the $\nu = 2$ step reappears. The absence of a $\nu = 2$ step is unusual for the 2D case, but can be interpreted here as a crossing of spin-split Landau levels of the first and second subbands. These changes illustrate how the integer quantum Hall effect occurs in a thick layer of electron gas with more than one subband occupied.

Measurements of the longitudinal magnetoresistance R_{zz} for the same sample at T = 50 mK with the magnetic field oriented parallel to the current direction are shown in Figs. 3a to 3e after progressively longer periods of illumination, which approximate'y correspond to the range between Figs. 2a and 2b. The presence of Shubnikov de

Haas oscillations in the longitudinal magnetoresistance at low magnetic fields shown in Fig. 3 is direct evidence that more than one subband of the well is occupied. Yoshino et. al.[7] have studied how the energy levels of a square well shift with a longitudinal magnetic field. They find that the nth subband of a square quantum well $E_n = n^2E_1$ at low field becomes the (n - 1)th Landau level $(n - 1/2)\hbar\omega_c/2\pi$ at high fields of a fan originating from an energy E_1 below the lowest subband at zero field. A peak in the longitudinal magnetoresistance is expected whenever the Fermi energy crosses one of these subbands; thus the number and location of peaks in R_{zz} determines the subband occupation in the longitudinal orientation. Note that a given subband empties at different fields for the longitudinal and the transverse orientations, because the total energy is different for these two cases[7]. Before illumination, in Fig. 3a, one peak is observed in the longitudinal magnetoresistance at $H \cong 0.7$ Tesla, indicating that two subbands are occupied in the well as grown.

For a parabolic well, the number of occupied subbands is expected to increase with illumination, while the Fermi energy remains essentially constant. This occurs as the width w_e of the electron layer increases and the energy scale $E_1 \propto 1/w_e^2$ of the spectrum decreases, introducing new subbands below E_F. These characteristics are confirmed by the longitudinal magnetoresistance data in Fig. 3. After increasing periods of illumination in Figs. 3b to 3e, the peak in Fig. 3a remains near the field $H \cong 0.8$ Tesla. This is evidence that the Fermi energy changes relatively little, because the energy of a filling subband is rapidly dominated by the magnetic term which does not change with E_1. A second peak appears in Fig. 3d at $H \cong 0.3$ Tesla after a period of illumination comparable to that for Fig. 2b. This indicates that a third subband has been introduced below the Fermi energy as expected for an increase in width of the electron layer.

These data demonstrate that the parabolic well technique[2,4] can be used to create thick layers of dense, high mobility electron gas. As the number of occupied subband increases, we observe characteristic changes in the integer quantum Hall effect.

Acknowledgement - We thank B.I. Halperin for helpful discussions. This research was supported in part by the National Science Foundation under grants DMR-85-08733 and DMR-86-14003.

REFERENCES

1. See for example R.E. Prange and S.M. Girvin eds., The Quantum Hall Effect (Springer Verlag, New York, 1987).

2. B.I. Halperin, Japan J. of Appl. Phys. 26, Suppl. 26-3, 1913 (1987).

3. H.L. Störmer, J.P. Eisenstein, A.C. Gossard, W. Weigmann, and K. Baldwin, Phys. Rev. Lett. 56, 85 (1986).

4. M. Sundaram, A.C. Gossard, J.H. English, and R.M. Westervelt, Superlattices and Microstructures, in press.

5. E.G. Gwinn, P.F. Hopkins, A.J. Rimberg, R.M. Westervelt, M. Sundaram and A.C. Gossard, in High Magnetic Fields in Semiconductor Physics II, ed. G. Landwehr (Springer Verlag, New York, 1988) in press.

6. M. Shayegan, T. Sajoto, M. Santos and C. Silvestre, Appl. Phys. Letters, in press.

7. J. Yoshino, H. Sakaki and T. Hotta, Surface Science 142, 326 (1984).

FIGURE CAPTIONS

Fig. 1 Schematic illustration of the conduction band edge vs. position for a parabolic well structure.

Fig. 2 Integer quantum Hall effect in a wide parabolic well: transverse magnetoresistance and Hall resistance (a) before illumination, areal density $n_H = 0.78 \times 10^{11} cm^{-2}$; (b) after illumination, $n_H = 1.12 \times 10^{11}$ cm^{-2}.

Fig. 3 Longitudinal magnetoresistance for a parabolic well (a) before illumination, density $n_H = 0.78 \times 10^{11} cm^{-2}$, and after illumination (b) $n_H = 0.95 \times 10^{11}$ cm^{-2}; (c) $n_H = 1.07 \times 10^{11} cm^{-2}$; (d) and (e) $n_H \cong 1.12 \times 10^{11} cm^{-2}$.

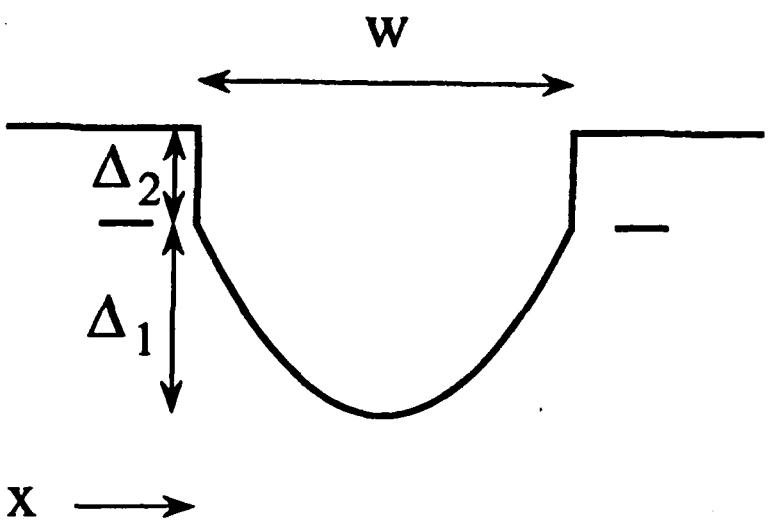

(a) empty

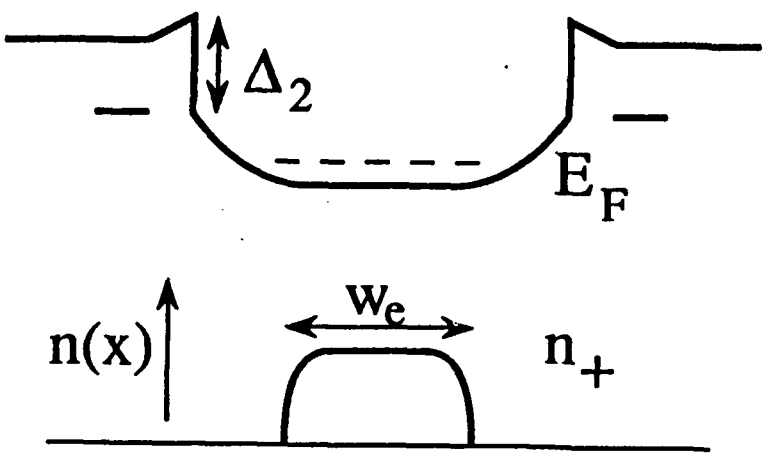

(b) partially full

Fig. 1

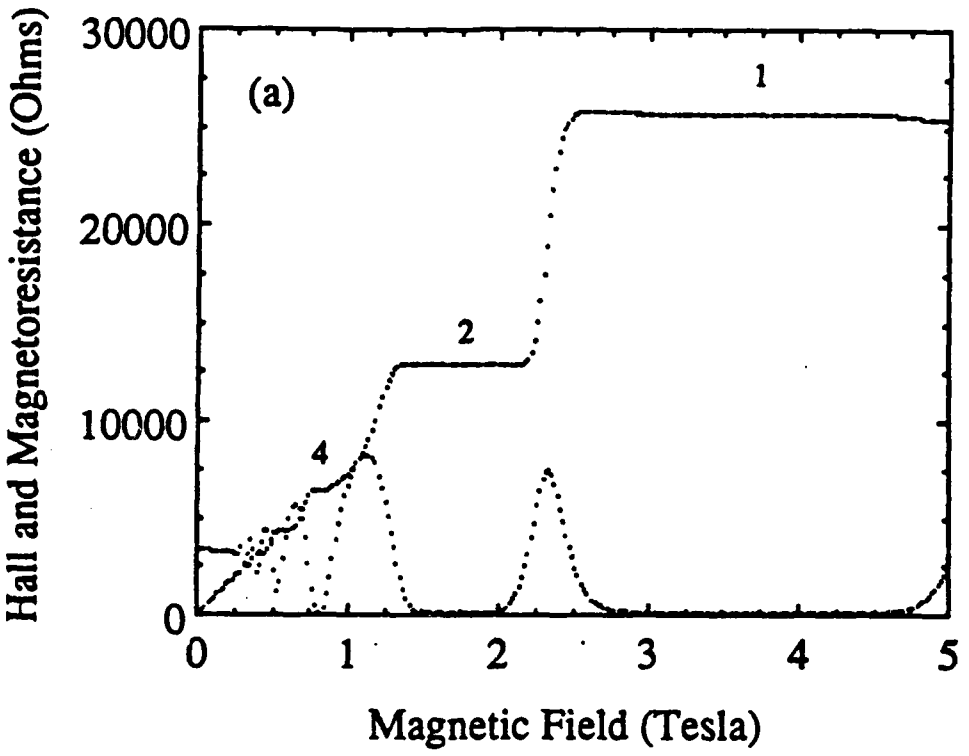
(a)
30000
20000
10000
0
Hall and Magnetoresistance (Ohms)
1
2
4
0
1
2
3
4
5
Magnetic Field (Tesla)

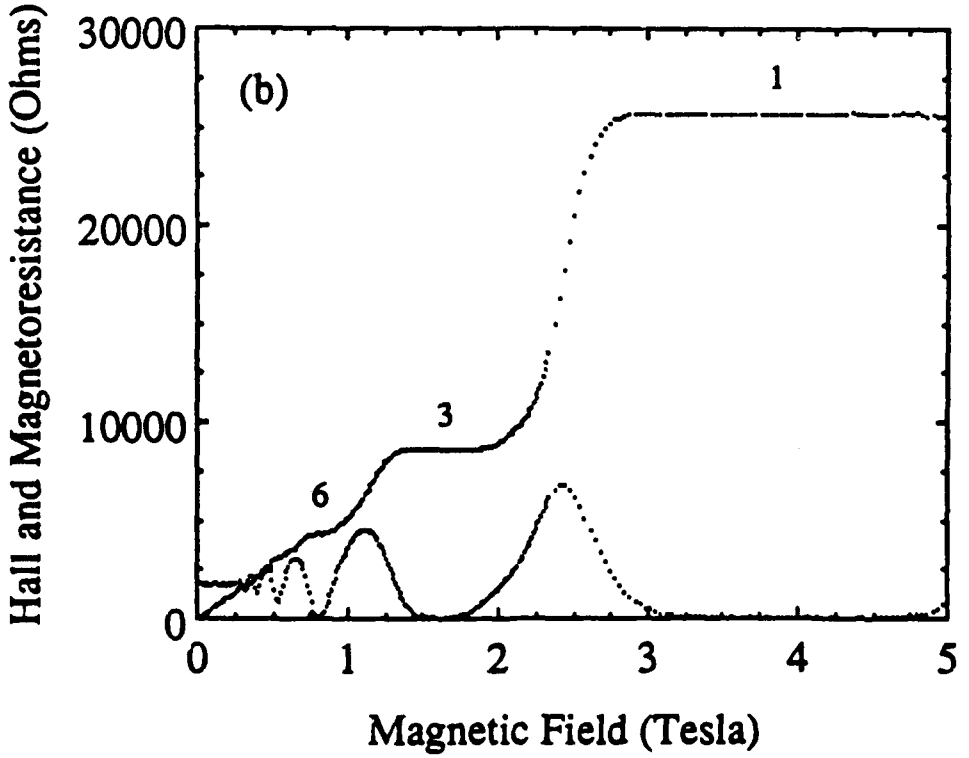
(b)
30000
20000
10000
0
Hall and Magnetoresistance (Ohms)
1
3
6
0
1
2
3
4
5
Magnetic Field (Tesla)

Fig. 2

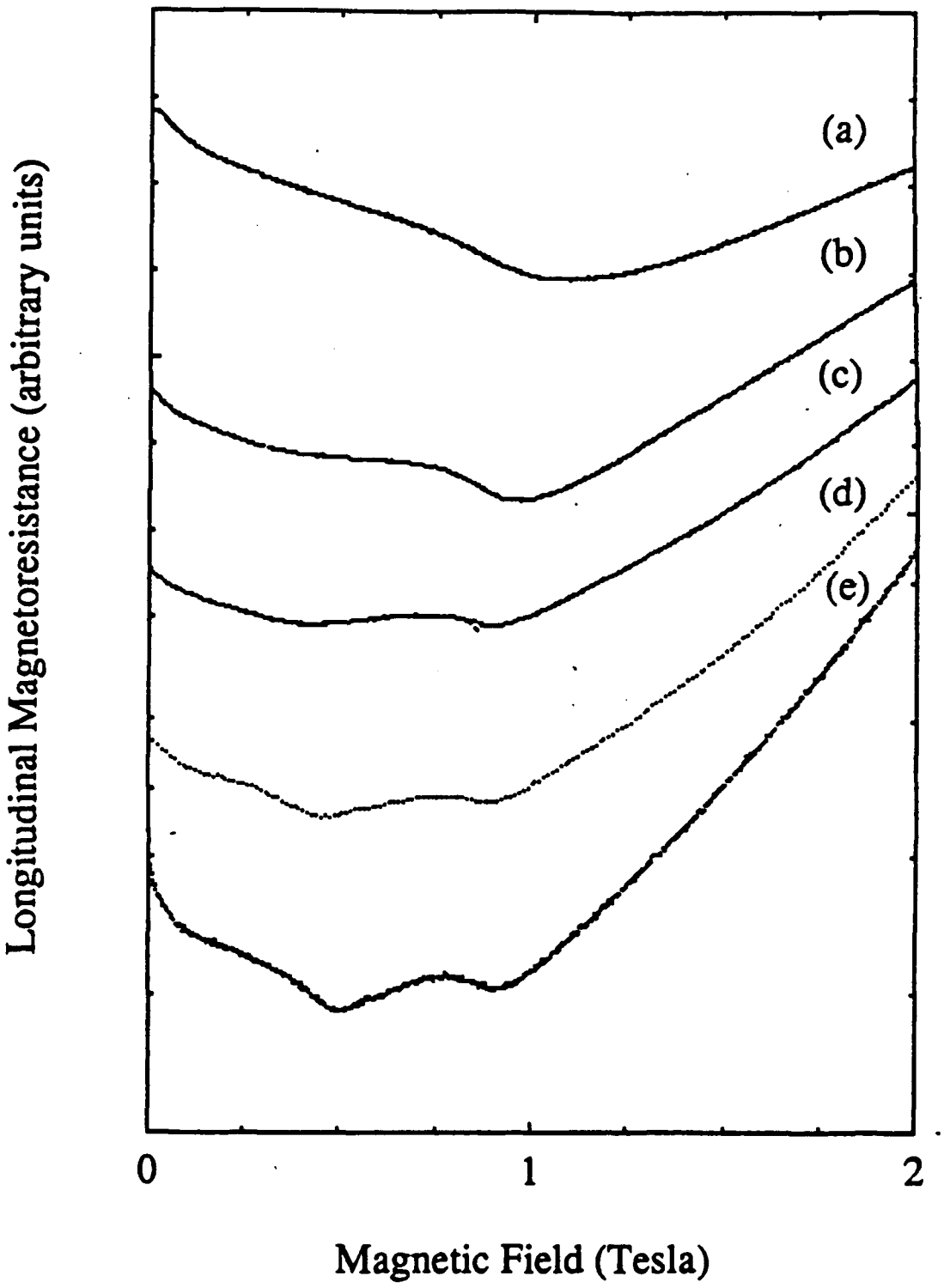
Longitudinal Magnetoresistance (arbitrary units)
(a)
(b)
(c)
(d)
(e)
0
1
2
Magnetic Field (Tesla)

Fig.3

Quantum Hall Effect in Wide Parabolic GaAs/$Al_xGa_{1-x}As$ Wells

E.G. Gwinn, R.M. Westervelt, P.F. Hopkins, and A.J. Rimberg
Division of Applied Sciences and Department of Physics
Harvard University, Cambridge MA 02138

M. Sundaram and A.C. Gossard
Department of Electrical and Materials Engineering
and Materials Department
University of California at Santa Barbara

P.A.C.S. nos. 72.20.My, 73.20.Dx, 71.25.Hc

received ( )

Parabolic GaAs/$Al_xGa_{1-x}As$ wells are used to create thick (> 1000 Å) spatially uniform layers of electron gas with low temperature mobility μ = (0.2 to 2.5)x10^5 cm^2/Vsec. These structures exhibit both the integer and fractional quantum Hall effect. Measurements of the integer quantum Hall effect in a 4000 Å wide parabolic well as the well is partially filled with electrons are used to study the transition from two toward three dimensional behavior.

A three dimensional electron gas in a strong magnetic field at low temperatures is predicted to show interesting phenomena when the electronic charge is cancelled by a uniform positive background. These include the quantum Hall effect[1,2] and possible collective electronic states[3]. Because electrons in doped semiconductors interact strongly with the background of positive point charges, producing magnetic freezeout, unambiguous experimental tests of these predictions have been difficult to make[3].

Remotely doped parabolic GaAs/$Al_xGa_{1-x}As$ wells can be used to create relatively thick (> 1000 Å) layers of electron gas[3-7] with low temperature mobility as high as[5] $\mu = 2.5 \times 10^5$ $cm^2/Vsec$, which do not freeze out in strong magnetic fields[5]. These structures show both the integer[5-7] and fractional[5] quantum Hall effect. In this letter we report magnetotransport measurements on a 4000 Å wide parabolic well as it is partially filled with electrons using persistent photoconductivity. The data show that the well fills at constant Fermi energy via an increase in width as expected for a spatially uniform slab of constant density, and they show how the integer quantum Hall effect changes in the transition away from two dimensions as the slab becomes thicker.

Figure 1 illustrates the conduction band edge vs. position for empty and partially filled parabolic wells[4]. For the empty well in Fig. 1a the parabolic potential of depth Δ_1 is confined by a

barrier of height Δ_2. Remotely located dopant layers on both sides are used to fill the well with electrons. The parabolic potential in Fig. 1a is identical to that produced by a three dimensional (3D) spatially uniform slab of positive charge of density $n_+ = 2\varepsilon\Delta_1/\pi e^2 w^2$. The electrons act to screen this fictitious charge as they enter the well. When the well is full, the electron density n is constant and equal to the design density n_+ in the limit that many electric subbands are occupied. The total self-consistent potential is then just that of a square well of width w and depth Δ_2. Even when the well is partially full, as in Fig. 1b, the electrons screen the parabolic potential and create a thinner slab of comparable density $n \cong n_+$ over part of the width w_e as indicated. As the well fills with electrons, the width w_e of the electron layer increases while the density and the Fermi energy E_F remain approximately constant. This process is self correcting and does not require precise control of the doping to create spatially uniform electron density profiles. These concepts are general[4], and can be used to create density profiles other than those in Fig. 1.

It is also interesting to consider filling of a parabolic well when the number of occupied subbands is not large, as for the experiments presented here. For a wide well partially filled with a dense electron gas, the electrostatic energy is typically much larger than the kinetic energy (Δ_1 = 150 meV, and E_F = 2.8 meV for

the data below). The electronic wavefunctions $\psi_i(z)$ thus tend to flatten at the expense of additional kinetic energy in order to produce a more uniform charge distribution and reduce the pseudo electrostatic energy[8]. For example, n(z) in Fig. 1b could also illustrate the spatial profile of the charge density when only one subband is occupied. As for the semiclassical case, this process is self correcting, and can be used to produce other wavefunction profiles.

The energy spectrum E_j of a partially filled parabolic well roughly approximates that of a square well $E_{Sj} = j^2 E_o$ of width w_e equal to that of the electron layer, with $E_o = (h/w_e)^2/8m_e$ and $m_e = 0.067\ m_o$. However, when only a few subbands are occupied, their energies are significantly shifted upward due to the increased kinetic energy associated with bending and flattening the wavefunction[8]. When more than one subband is occupied, filling of the well is expected to occur at approximately constant Fermi energy $E_F - E_1$, corresponding to constant density, while the separation between two given subbands decreases as the electron layer becomes wider. The number of occupied subbands increases while the Fermi energy remains approximately constant.

We have studied five parabolic well structures with low temperature Hall mobilities between $\mu_H = 2\times10^4$ cm^2/Vsec and $\mu_H = 2.5\times10^5$ cm^2/Vsec, and with widths from w = 1000 Å to w = 4000 Å. We present data here for a 4000 Å well with

μ_H = 5x10^4 cm^2/Vsec and design parameters Δ_1 = 150 meV (for which n_+w = 2.2x10^{11} cm^{-2}) and Δ_2 = 75 meV. These structures were grown[4] using molecular beam epitaxy on semi-insulating GaAs substrates. The parabolic potential was created by changing the relative thickness of alternating GaAs and $Al_{0.3}Ga_{0.7}As$ layers in a fine superlattice of period 20 Å so that the average Al concentration varied parabolically from x = 0 in the center to x = 0.2 at the edge of the well. Electrons were deposited in the well from Si doped layers symmetrically set back 200 Å from both sides of the well in the $Al_{0.3}Ga_{0.7}As$ barrier.

Photolithographically defined Hall bars with dimensions 0.5mmx5mm were prepared with In electrical contacts, produced by baking for 5 minutes at 400 °C in a reducing atmosphere. The samples were mounted stress free and cooled slowly in the dark in a dilution refrigerator equipped with a 7 Tesla superconducting solenoid. Measurements of the transverse Hall and magnetoresistance R_{xy} and R_{xx} with the magnetic field perpendicular to the plane of the sample, and the longitudinal magnetoresistance R_L with an in plane magnetic field, were made using lockin techniques and recorded in a computer; typical values of the applied current were I ~ 30 nA. Between the transverse and longitudinal data sets below, the sample was warmed to room temperature for remounting. The measured low temperature areal Hall density was n_H = 0.78x10^{11} cm^{-2} before illumination,

indicating that the well was roughly 1/3 full as grown with $n_H/n_+w = 0.36$. Electrons were added to the well by illuminating the sample *in situ* in zero magnetic field with a light-emitting diode.

Measurements of the longitudinal magnetoresistance R_L with the magnetic field in the plane of the sample and parallel to the current direction were used to determine the number of occupied subbands. Figure 2 illustrates the magnetic field dependence of the bottoms E_j of the subbands of a square well[9] with an in plane magnetic field H, for two different energy level separations, adjusted to fit the data shown in Figs. 3 to 5 below. The energies E_j smoothly change from the energy levels of a square well $E_{Sj} = j^2(h/w_e)^2/8m_e$ to the corresponding levels of a Landau fan $E_{Hj} = [(j - 1) + 1/2]h\omega_c/2\pi$ as H increases[9]. For purposes of illustration, the interpolation formula $E_j = (E_{Sj}^2 + E_{Hj}^2)^{1/2}$ is shown in Fig. 2; numerical calculations[9] for square wells yield similar results for E_j. Transverse Shubnikov de Haas measurements for low magnetic fields (see Fig. 4 below) show that the Fermi energy $E_F - E_1 = 2.8$ meV in Figs. 2a and 2b remains nearly constant as the well is filled. Following Yoshino et. al.[9] we associate each peak in R_L with a crossing between E_F and the bottom of a subband E_j with $j > 1$. The use of another point on the oscillation (for example dips) does not qualitatively change our conclusions.

Longitudinal magnetoresistance data taken at T = 50 mK are shown in Fig. 3a before illumination, and in Figs. 3b and 3c after increasing periods of illumination. The data before illumination in Fig. 3a show a single peak in R_L near H = 0.7 Tesla indicating the transition from two occupied subbands to one, as illustrated in Fig. 2a. As electrons are added to the well in Figs. 3b and 3c, this peak moves relatively little as expected for constant Fermi energy, and a new peak is introduced at lower fields corresponding to the transition from three to two occupied subbands (Fig. 2b). These data demonstrate that two subbands of the well are occupied as grown, and confirm that a parabolic well fills with electrons by decreasing the separation of the subbands while the Fermi level $E_F - E_1$ remains relatively constant.

Figures 4 and 5 present measurements of the transverse Hall and magnetoresistance R_{xy} and R_{xx} at T = 50 mK after increasing periods of illumination approximately corresponding to the range in Figs. 3a to 3c, based on the resistance R_o in zero magnetic field. The Shubnikov-de Haas oscillations in R_{xx} shown in Fig. 4 show that the Fermi energy $E_F - E_1 = 2.8 \pm 0.1$ meV remains essentially constant as electrons are added to the well, while the zero field resistance drops by a factor ~ 2 and the number of occupied subbands increases from 2 to 3. This Fermi energy is larger than one would naively expect for a square well of width $w_e \sim n_H/n_+ \sim 1500$ Å corresponding to the measured Hall density.

We attribute the difference in part to an increase in energy spacing of the subbands due to distortion of the wavefunctions in order to minimize their electrostatic energy, as described above.

The low field Hall resistance R_{xy} in Figs. 4a to 4c decreases continuously with illumination and exhibits quantum Hall effect steps. The measured areal Hall density n_H increased with illumination from $n_H = 0.78 \times 10^{11}$ cm^{-2} to $n_H = 1.12 \times 10^{11}$ cm^{-2} over the range shown in Figs. 4a to 4c. Because few subbands are occupied, n_H underestimates the true areal density n_s; higher subbands with lower mobility contribute relatively less to n_H [10]. A plot of n_H vs. R_O flattens near $R_O \sim 2000\ \Omega$, before the illumination corresponding to occupation of a third subband in Fig. 3c.

Figures 4 and 5 display well developed quantum Hall plateaus $R_{xy} = h/\nu e^2$ at integer filling factors ν. The magnetoresistance R_{xx} approaches zero at Hall steps both before and after illumination, evidence against the possible formation of parallel conduction paths. A plot of the Landau levels for the transverse case neglecting spin splitting is shown for comparison in Figs. 6a and 6b: the electric subband energies and the Fermi energy $E_F - E_1$ shown are the same as for Figs. 2a and 2b respectively, and they correspond approximately to the range of illumination for the transverse data. Whenever the Fermi energy lies in a band of localized states between Landau levels, a quantum Hall step will

occur with filling factor ν equal to the number of spin split Landau levels below E_F, according to conventional theory[1].

Figures 4 and 5 demonstrate how the quantum Hall effect changes in the transition from two toward three dimensions as the electron layer becomes thicker and more subbands are occupied. Before illumination in Fig. 5a, well developed Hall plateaus are seen in the data for $\nu = 1$, 2 and 4. Comparison with Fig. 6a suggests that these are for the two dimensional case with only the lowest electric subband occupied. As the number of electrons in the well is increased in Figs. 5b and 5c, an additional Hall step appears at $\nu = 3$, and the step at $\nu = 2$ weakens and disappears entirely. Comparison with Fig. 6b suggests that this change is caused by the introduction of a spin split Landau level from the second subband below the Fermi level. After additional illumination the $\nu = 2$ step reappears. Over the same range of illumination in Figs. 4a to 4c and in Figs. 5a to 5c, the $\nu = 4$ step first disappears, then reappears as a $\nu = 6$ step at the same magnetic field, due to the introduction of an unsplit Landau level from the second subband beneath the Fermi energy (Fig. 6). Thus the location of the quantum Hall steps remains fixed due to the constant Fermi energy, while the filling factor increases with thickness of the electron layer. In the conventional picture[1] quantum Hall steps disappear for a sufficiently thick electron layer when the cores of extended states from the corresponding Landau levels overlap.

We thank B.I. Halperin for many helpful discussions and J.H. English for help in sample preparation. This work was supported in part by the National Science Foundation under grants DMR-85-08733 and DMR-86-14003.

REFERENCES

1. Reviewed in R.E. Prange and S.M. Girvin eds., The Quantum Hall Effect (Springer Verlag, New York, 1987).

2. Observed in a thick layered heterostructure by H.L. Störmer, J.P. Eisenstein, A.C. Gossard, W. Weigmann, and K. Baldwin, Phys. Rev. Lett. 56, 85 (1986).

3. Reviewed in B.I. Halperin, Japan J. of Appl. Phys. 26, Suppl. 26-3, 1913 (1987).

4. M. Sundaram, A.C. Gossard, J.H. English, and R.M. Westervelt, Superlattices and Microstructures, in press.

5. E.G. Gwinn, P.F. Hopkins, A.J. Rimberg, R.M. Westervelt, M. Sundaram and A.C. Gossard, in High Magnetic Fields in Semiconductor Physics II, ed. G. Landwehr (Springer Verlag, New York, 1988) in press.

6. E.G. Gwinn, R.M. Westervelt, P.F. Hopkins, A.J. Rimberg, M. Sundaram, and A.C. Gossard, Superlattices and Microstructures, in press.

7. M. Shayegan, T. Sajoto, M. Santos and C. Silvestre, Appl. Phys. Letters, in press.

8. A simple uncertainty principle calculation using a trapezoidal charge density $\rho(z)$ of half width w_e and transitional thickness a gives $a \sim (5h^2/2m_e^2\omega_p^2)^{1/4}$ independent of w_e and zero point energy $E \sim (w_e/a)E_{S1}$ with $\omega_p^2 = 4\pi n_+ e^2/\varepsilon m_e$ and $E_{S1} = h^2/8m_e w_e^2$. For the 4000 Å well as grown, $a \sim 600$ Å and $E/E_{S1} \sim 2$ to 3, using $w_e = 1400$ Å and $n_+ = 5.5\times10^{15}$ cm^{-3}.

9. J. Yoshino, H. Sakaki and T. Hotta, Surface Science 142, 326 (1984).

10. H.L. Störmer, A.C. Gossard, and W. Wiegmann, Solid State Commun. 41, 707 (1982).

FIGURE CAPTIONS

Fig. 1 Schematic illustration of the conduction band edge vs. position for a parabolic well (see text).

Fig. 2 Longitudinal subband energies vs. magnetic field for square wells of increasing thickness: (a) $E_2 - E_1 = 2.25$ meV, (b) $E_2 - E_1 = 0.95$ meV. The zero field Fermi energy $E_F - E_1 = 2.8$ meV is indicated in both (a) and (b).

Fig. 3 Longditudinal magnetoresistance: (a) before illumination, zero field resistance $R_o = 3650\ \Omega$, (b) after illumination: $R_o = 2050\ \Omega$, (c) $R_o = 1500\ \Omega$.

Fig. 4 Transverse Hall and magnetoresistance: (a) before illumination, $R_o = 3540\ \Omega$, after illumination: (b) $R_o = 2120\ \Omega$, (c) $R_o = 1800\ \Omega$.

Fig. 5 Transverse Hall and magnetoresistance: (a) before illumination, $R_o = 3540\ \Omega$, after illumination: (b) $R_o = 2120\ \Omega$, (c) $R_o = 1800\ \Omega$.

Fig. 6 Transverse Landau levels for square wells of increasing thickness: (a) $E_2 - E_1 = 2.25$ meV, (b) $E_2 - E_1 = 0.95$ meV. The zero field Fermi energy $E_F - E_1 = 2.8$ meV is indicated in both (a) and (b).

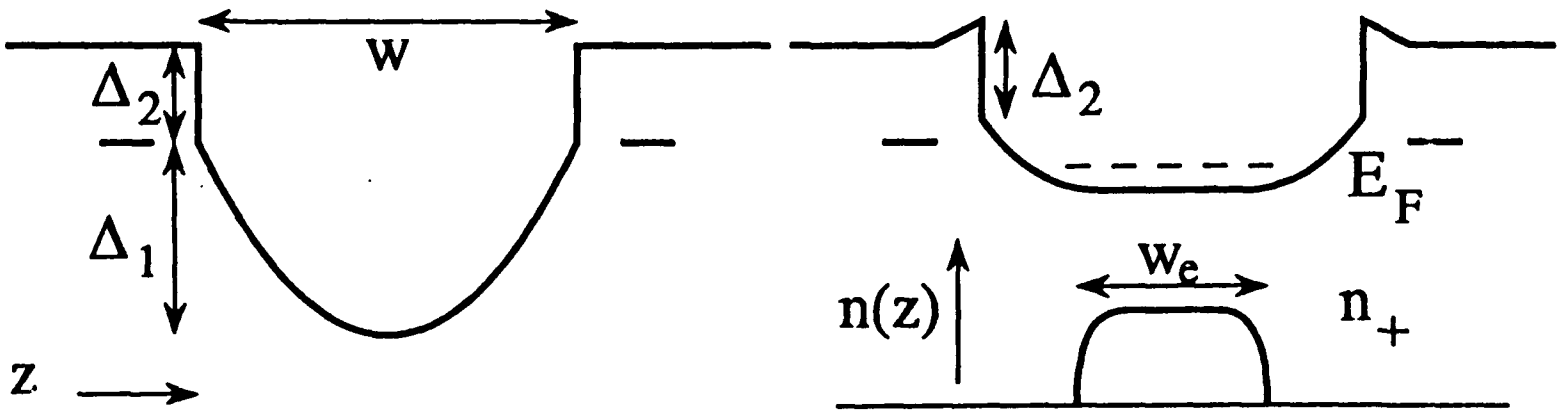

(a) empty (b) partially full

Fig. 9.1

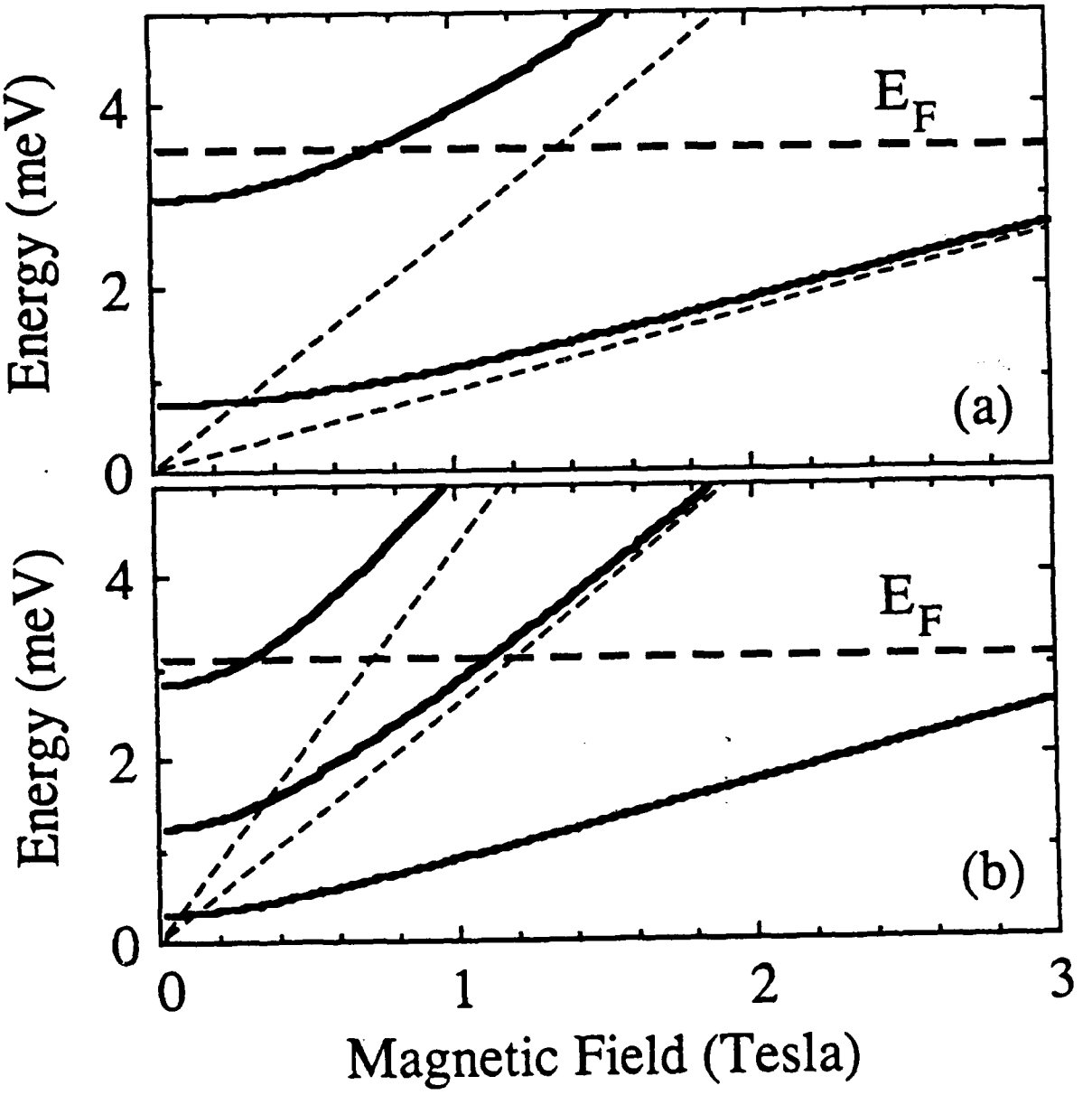
Energy (meV)
4
2
0
E_F
(a)
Energy (meV)
4
2
0
E_F
(b)
0
1
2
3
Magnetic Field (Tesla)

Fig. 2

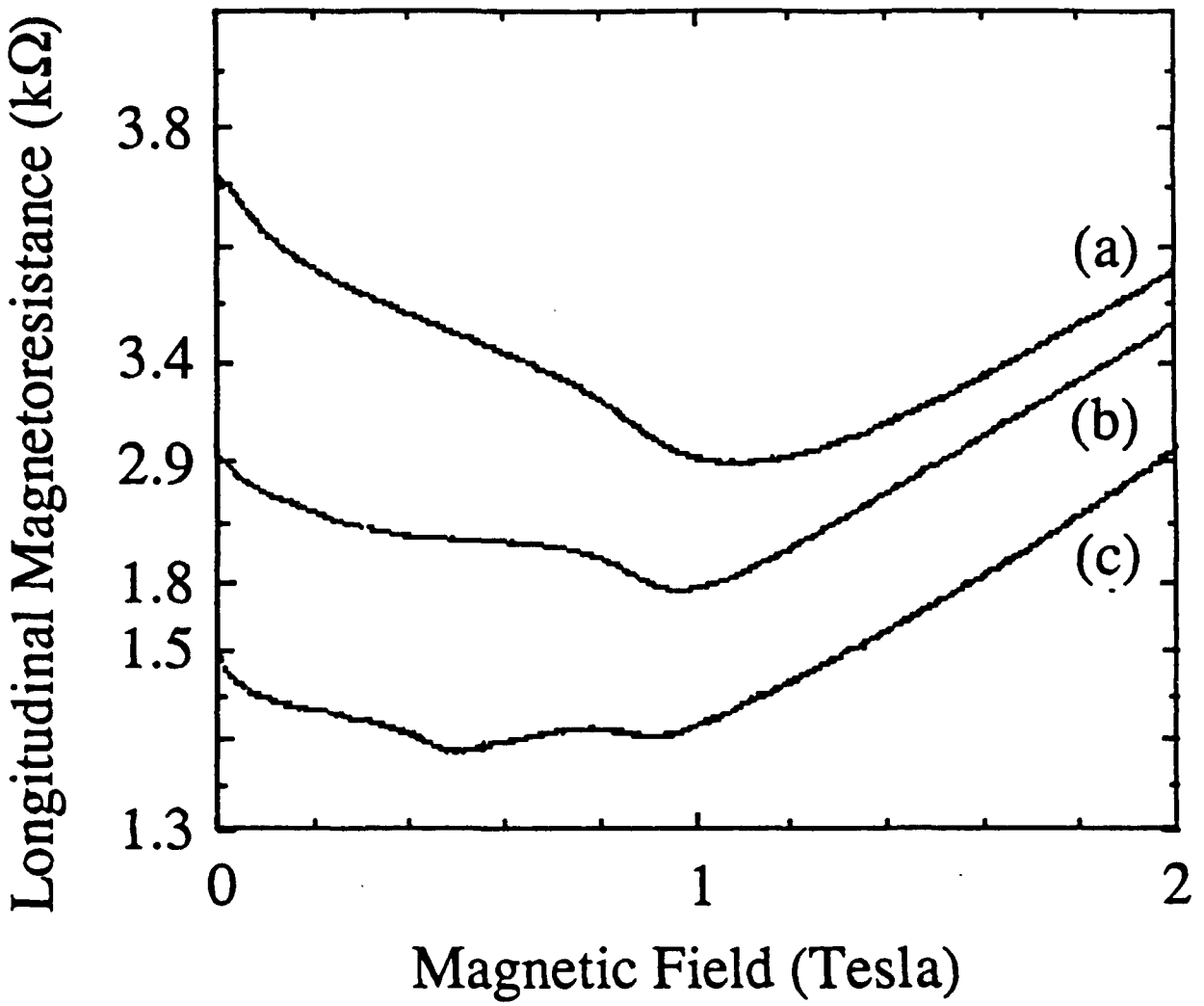
Longitudinal Magnetoresistance (kΩ)
3.8
3.4
2.9
1.8
1.5
1.3
0
1
2
Magnetic Field (Tesla)
(a)
(b)
(c)

Fig. 3

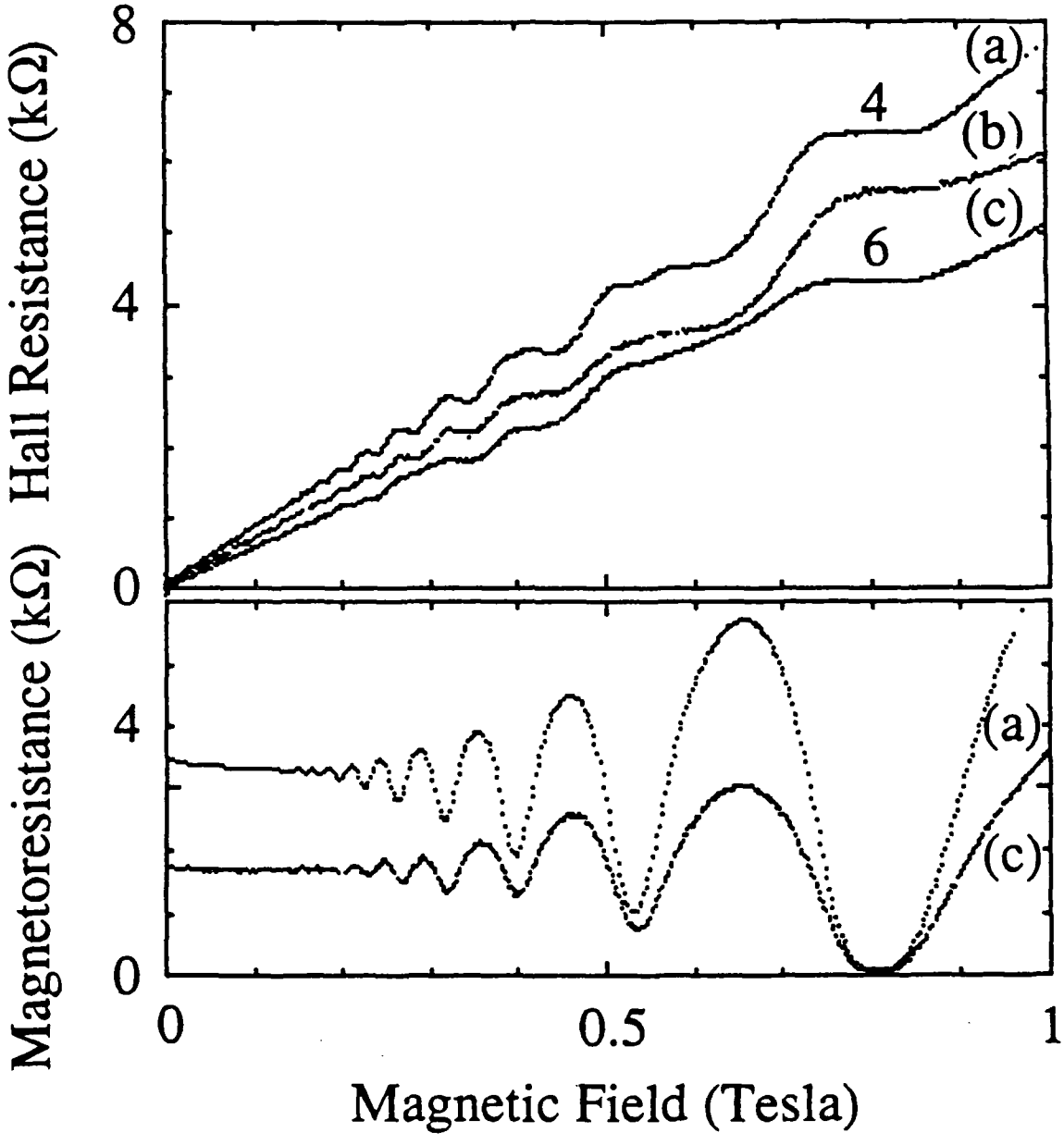
Magnetoresistance (kΩ) Hall Resistance (kΩ)
8
4
0
(a)
4
(b)
(c)
6
4
0
(a)
(c)
0
0.5
1
Magnetic Field (Tesla)

Fig. 4

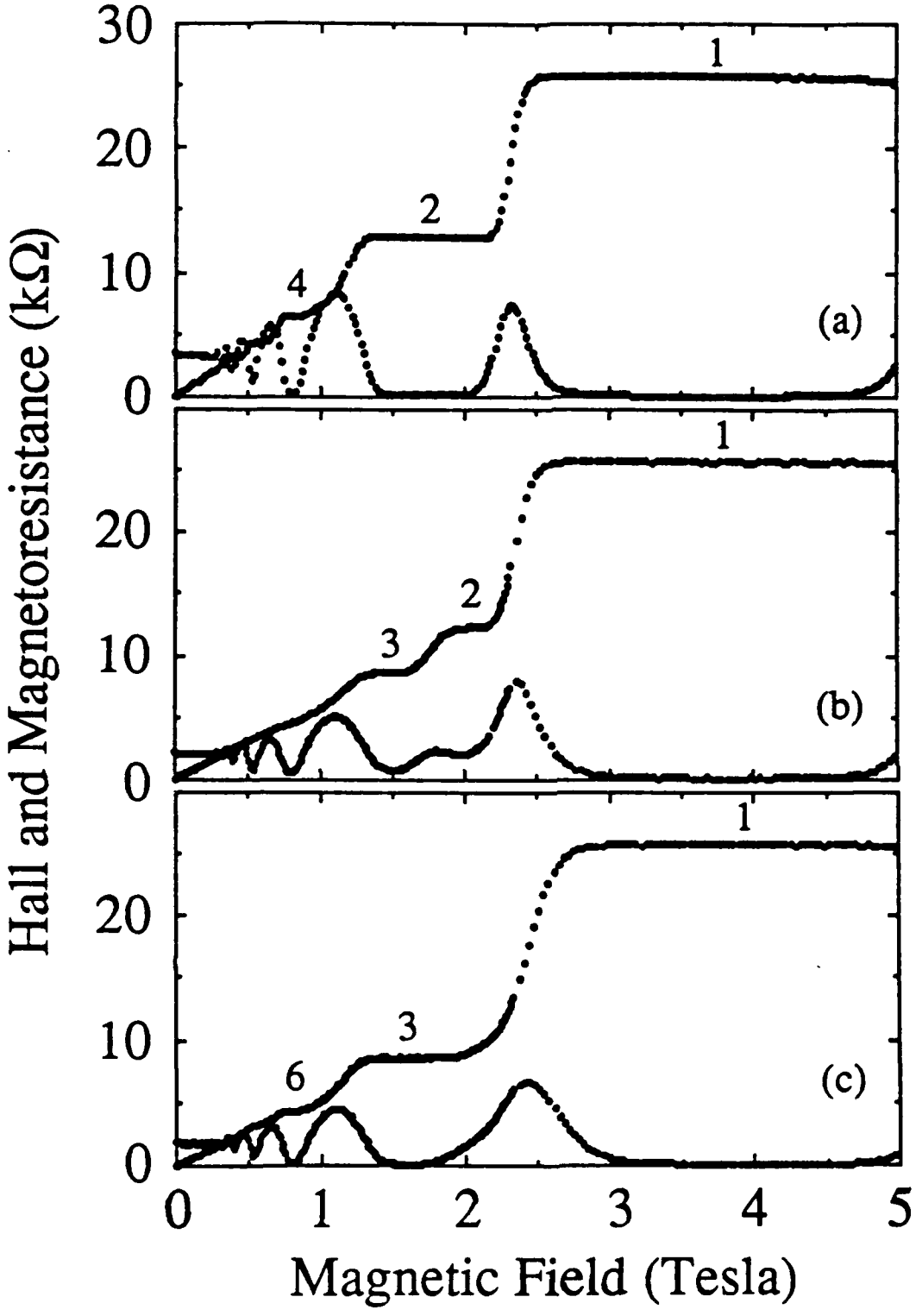
Hall and Magnetoresistance (kΩ)
30
20
10
0
1
2
4
(a)
1
20
2
3
10
(b)
0
1
20
3
6
10
(c)
0
0
1
2
3
4
5
Magnetic Field (Tesla)

Fig.5

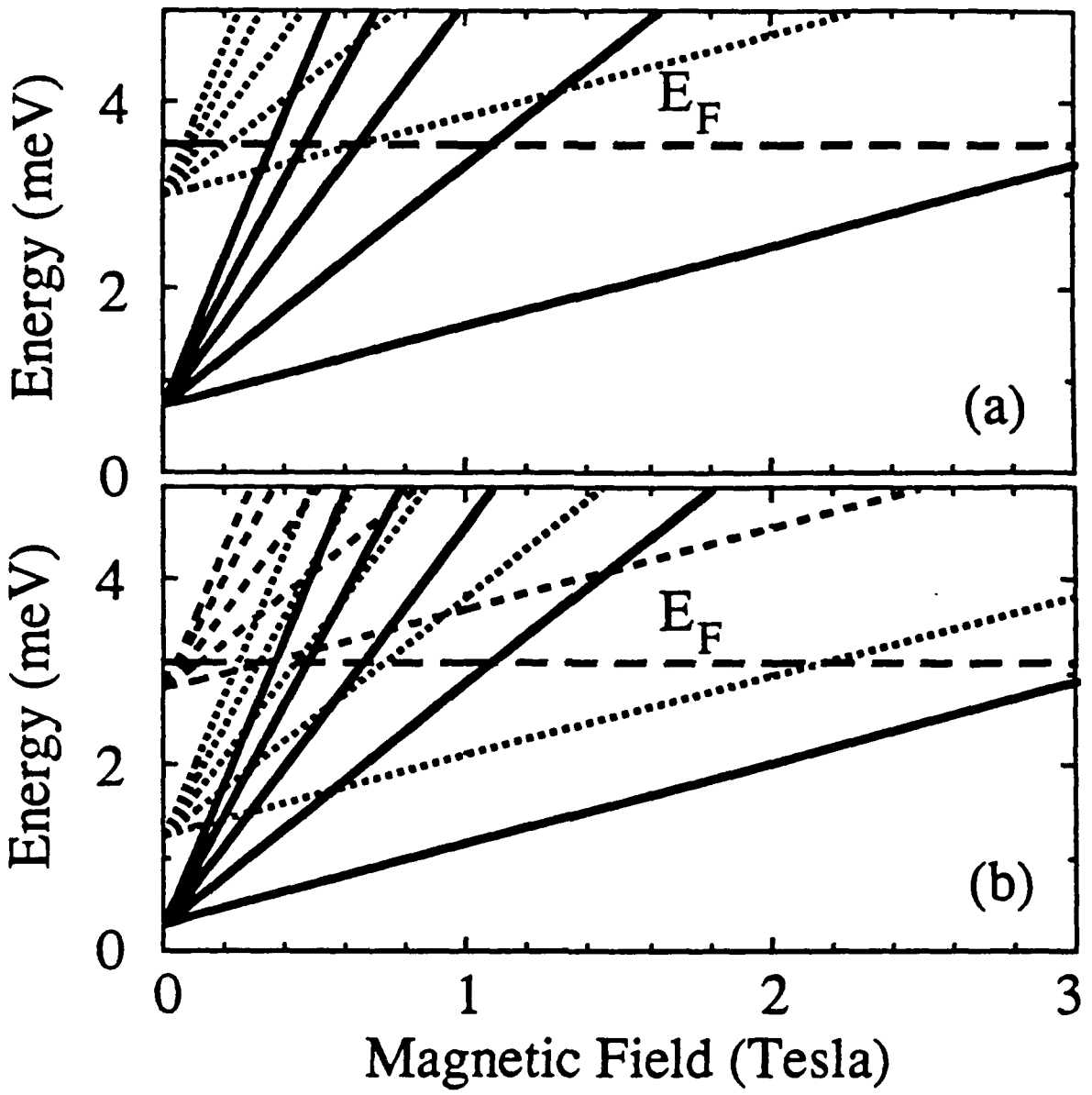
Energy (meV)
4
2
0
E_F
(a)
Energy (meV)
4
2
0
E_F
(b)
0
1
2
3
Magnetic Field (Tesla)

Fig. 6

High Magnetic Fields in Semiconductor Physics II, ed. G. Landwehr, Springer Series on Solid State Sciences (Springer Verlag, New York)

Quantum Hall Effect in Wide Parabolic GaAs/$Al_xGa_{1-x}As$ Wells

E.G. Gwinn, P.F. Hopkins, A.J. Rimberg, and R.M. Westervelt
Division of Applied Sciences and Department of Physics
Harvard University, Cambridge MA 02138

M. Sundaram and A.C. Gossard
Department of Electrical and Computer Engineering and
Materials Department
University of California, Santa Barbara, CA 93106

1. INTRODUCTION

The ability to produce narrow two-dimensional (2D) layers of high mobility electron gas in semiconductor structures has permitted the study of the 2D electron gas in strong magnetic fields under nearly ideal conditions, and led to the discovery of the integer and fractional quantum Hall effects [1]. Despite many interesting experiments, comparable progress has not been made for the three dimensional (3D) electron gas in semiconductors, due in part to the strong influence of the potential from dopant atoms. Remotely-doped parabolic GaAs/$Al_xGa_{1-x}As$ wells can be used to produce relatively thick (>1000 Å) layers of high mobility electron gas [2,3] which are spatially uniform due to the action of the parabolic potential. We report here high magnetic field measurements of both the 2D integer and fractional quantum Hall effects for a partially-filled wide parabolic GaAs/$Al_xGa_{1-x}As$ well [2] with very high low temperature mobility $\mu = 2.5 \times 10^5$ $cm^2/Vsec$. These measurements demonstrate both the feasibility of the parabolic well technique and the high quality of the structures.

2. DENSE ELECTRON GAS IN WIDE PARABOLIC WELLS

Figure 1 is a schematic illustration of the conduction band edge vs. position for empty and partially-filled parabolic wells. For the empty well in Fig. 1a, the parabolic potential of depth Δ_1 is confined by a barrier of height Δ_2. Remotely located dopant layers in the barrier are used to fill the well with electrons. The essential idea needed to understand the filling of the well is that the parabolic potential is identical to that produced by a spatially-uniform positively charged background of 3D density $n_+ = 2\varepsilon\Delta_1/\pi e^2 w^2$. The electrons act to screen this fictitious positive charge as they enter the well. When the well is full, the electron density n is constant and equal to the design density n_+ over the entire width of the well, and the total potential is simply that of a square well of width w and depth Δ_2. Even when the well is partially full, as in Fig. 1b, the electrons act to screen the parabolic potential and create a thinner slab of comparable density $n \cong n_+$ over part of the width w_e as indicated. For this case the total potential is approximately that of a square well of width w_e. Thus this process is self correcting and does not require precise control

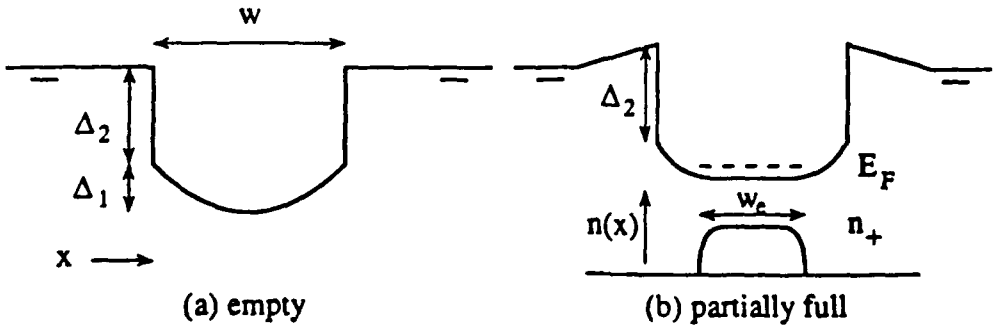

Fig. 1 Illustration of the spatial profile of the conduction band edge for (a) empty and (b) partially full parabolic wells

of the doping to generate spatially uniform electron density profiles. These concepts are completely general, and can be used to create density profiles other than those in Fig. 1.

Parabolic well heterostructures were grown [2] using molecular beam epitaxy on semi-insulating GaAs substrates. The parabolic potential was created by changing the relative thickness of alternating GaAs and $Al_{0.4}Ga_{0.6}As$ layers in a fine superlattice of period 20 Å, with a $Al_{0.4}Ga_{0.6}As$ barrier. Electrons were deposited in the well from Si-doped layers in the barrier symmetrically set back from both sides of the well. Five structures have been grown and characterized to date. For the structure discussed here the well parameters are: width $w = 2000$ Å, parabolic well depth $\Delta_1 = 155$ meV (for which $n_+ = 2.25 \times 10^{16}$ cm^{-3}), and barrier height $\Delta_2 = 143$ meV. Low field Hall effect measurements were used to determine the mobility $\mu = 2.5 \times 10^5$ cm^2/Vsec and the areal electron density $n_{2D} = 1.9 \times 10^{11}$ cm^{-2} at T = 1.5 K. These measurements indicate that the well is partially full with $w_e \sim n_{2D}/n_+ \equiv 800$ Å.

3. QUANTUM HALL EFFECT

Parabolic well samples were prepared in a Hall bar geometry defined using optical lithography. Electrical contacts were made by applying small amounts of In to the contact pads and baking at 400 C for ~ 5 min in a reducing atmosphere. The samples were mounted stress-free and immersed in liquid ^{3}He in a pumped ^{3}He cryostat. Strong magnetic fields to H ~ 20 Tesla were applied using a Bitter magnet, and the Hall resistance and transverse magnetoresistance were simultaneously measured and recorded using separate PAR 113 preamplifiers and a digital lock-in technique with a microcomputer. Typical values of the applied current were ~ 1 μA.

Figure 2 presents Hall effect and magnetoresistance data which clearly show both the integer and fractional quantum Hall effects. Here the Hall resistance and magnetoresistance measured at the temperature T = 0.5 K are plotted vs. magnetic

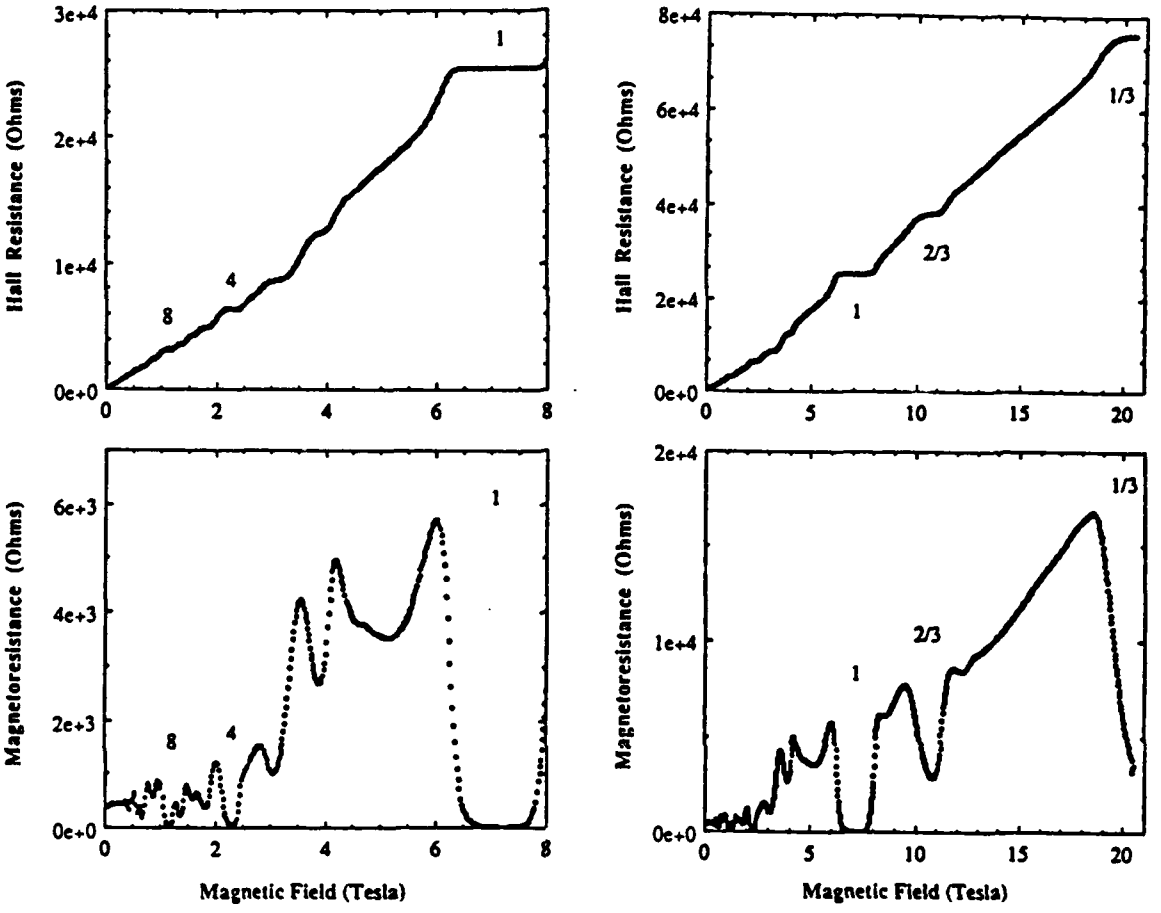

Fig. 2 Integer and fractional quantum Hall effect at T = 0.5 K for a partially-filled parabolic well in the two-dimensional high field limit

field H over the ranges 0 to 8 Tesla and 0 to 20 Tesla. Because the degeneracy of the lowest Landau level of the lowest sub-band of the well is sufficient to contain the measured areal density n_{2D} for H > 4 Tesla, the electron gas is expected to be two dimensional at moderately high fields. Well developed Hall plateaus for the integer quantum Hall effect are shown at filling factors ν = 1, 4 and 8 as indicated in Fig. 2, and indications of developing plateaus in both the Hall effect and magnetoresistance occur for ν = 2, 3, 5, 6, and 7. The Hall resistances and fields associated with these steps are in agreement with 2D theory. However, the Shubnikov-de Haas oscillations in the magnetoresistance at fields H < 1 Tesla are not simply periodic, suggesting that more than one sub-band may be occupied at the lowest fields. Plateaus are seen for the fractional quantum Hall effect at ν = 2/3 and ν = 1/3 (cut off by limit of the field sweep) and suggested at ν = 3/5 and 4/5, in agreement with 2D theory. The integer quantum Hall effect

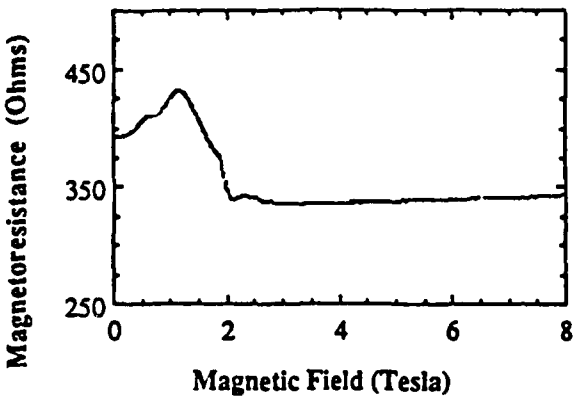

Fig. 3 Longitudinal magnetoresistance at T = 0.5 K

has also been observed at a higher temperature T = 1.5 K in samples from 3 of the 4 other parabolic well structures studied.

Figure 3 is a plot of the longitudinal magnetoresistance of the same sample at T = 0.5 K with the magnetic field parallel to the current direction. The presence of a Shubnikov-de Haas oscillation peak in Fig. 3 suggests that at least two sub-bands of the well are occupied below H ~ 1 Tesla. This result is consistent with the filling of a square well of width w_e by the measured areal density n_{2D}. The spectrum for this case is $E_n = n^2 E_o$ with $E_o \sim 0.8$ meV and the Fermi energy from n_{2D} is $E_F - E_o \sim 5$ meV, which predicts that two sub-bands are occupied.

4. ACKNOWLEDGEMENTS

We thank B.I. Halperin for many helpful discussions, and J.H. English for help in sample preparation. Part of this work was performed at the Francis Bitter National Laboratory supported at M.I.T. by the National Science Foundation. This research was supported in part by NSF grants DMR-85-08733 and DMR-86-14003.

REFERENCES

1. See for example R.E. Prange and S.M. Girvin eds.: The Quantum Hall Effect (Springer Verlag, New York, 1987)

2. M. Sundaram, A.C. Gossard, J.H. English, and R.M. Westervelt: Superlattices and Microstructures, in press

3. B.I. Halperin, Japan J. of Appl. Phys. 26, Suppl. 26-3, 1913 (1987)

CARD (CC 1-3): 2 3

NATIONAL AERONAUTICS AND SPACE ADMINISTRATION

NEW TECHNOLOGY TRANSMITTAL

(See Instructions on Reverse)

Approved Through January 1970
Budget Bureau No. 104-R0046

NT CONTROL NUMBER (CC 4-11): NPO-17754

1. TITLE
TUNABLE SUBMILLIMETER WAVE GENERATOR

2. INNOVATOR(S)
Joseph Maserjian
*Arthur C. Gossard

3. EMPLOYER (Organization and division)
Caltech/JPL
*University of California

4. ADDRESS (Place of performance)
4800 Oak Grove Dr., Pasadena, Ca. 91103
*Santa Barbara, CA

5. DOCUMENTATION (Full and complete disclosure must be enclosed, the contents of which are discussed in NHB 2170.3, Documentation Guidelines for New Technology Reporting. Place an "X" to the left of those items of documentation which are available but NOT enclosed with this transmittal)

	ENGINEERING SPECIFICATIONS		OPERATING MANUALS		COMPUTER TAPES/CARDS
	ASSEMBLY/MFG DRAWINGS		TEST DATA		
	PARTS OR INGREDIENTS LIST		ASSEMBLY/MFG PROCEDURES		

6. PREVIOUS PUBLICATION OR PUBLIC DISCLOSURE

PUBLICATION
TYPE: ☐ JOURNAL ☐ REPORT ☐ CONFERENCE OR SEMINAR
BY: ☐ NASA ☐ OTHER GOVT. ☐ CONTRACTOR ☐
VOLUME NO. | PAGE | DATE | STATUTORY BAR ESTABLISHED (Date)
TITLE

PATENT
STATUS: ☐ APPLICATION FILED ☐ ISSUED
NO. | DATE

7. STATE OF DEVELOPMENT

☐ CONCEPT ONLY ☐ DESIGN ☐ PROTOTYPE ☐ MODIFICATION ☐ PRODUCTION MODEL ☐ USED IN CURRENT WORK

8. ORIGIN (CC 12): P

9. NASA PRIME CONTRACT NO. (CC 13-23): NAS 7 - 918

10. SUBCONTRACT TIER (CC 24):

11. CONTRACTOR REPORTABLE ITEM NO. (CC 25-33): 17754

12. CONTRACTOR/GRANTEE NEW TECHNOLOGY Not SUBMITTED PURSUANT TO NT/PRI CLAUSE PROVISION (CC 34) ☐

For Internal Use Only

13. SUBCONTRACTOR CIC (CC 35-41):

14. NT RECEIPT DATE (CC 42-47): MO 04 DAY 05 YR 88

(RE-238)

15. PROJ. NO. (CC 48-51): -644

16. EVALUATION ORGANIZATION (CC 52-54): NPO

17. NT FORWARDED FOR EVALUATION (Date) (CC 55-60): MO DAY YR

18. COMMENTS
No additional material is available for a technical support package.

	NAME AND TITLE	SIGNATURE	DATE
19. PREPARED BY	Robert S. Jamieson Patent Agent		11/17/88
20. APPROVED (Center TUO)	NAME Gordon S. Chapman T. U. Officer	SIGNATURE	DATE

NASA FORM 666 SEP 68 PREVIOUS EDITIONS ARE OBSOLETE.

NEW TECHNOLOGY DATA SHEET

JPL CASE NO. 7256

SUBMITTED BY NAME'S

	FIRST INITIAL (LAST)	SECTION	EXT.	SUPERVISOR	Residence & Mailing Address	Citizenship
1)	Joseph (nmi) Maserjian* S.S. NO. 084-20-5219	346	43801	K.Koliwad	5668 Pine Cone Road La Crescenta, CA 91214	USA
2)	Arthur C. Gossard S.S. NO 028-26-0677	Univ. of Cal Barbara		@ Santa	675 Las Palmas Drive Santa Barbara, CA 93110	USA
3)	S.S NO.					
4)	*Temporarily at Univ. of Cal. @ Santa Barbara when invention was made					
	S.S NO.					

1. TITLE

TUNABLE SUBMILLIMETER WAVE GENERATOR

2. NOVEL FEATURES

A very high frequency local oscillator for heterodyne mixing comprises a plurality of parabolic quantum wells with energy levels resembling harmonic oscillator devices, wherein an electron current is introduced among the wells thereby accelerating the electrons into higher energy levels such that they emit monochromatic submillimeter wave radiation corresponding to transitions between the energy levels in a manner analogous to cyclotron emission without high magnetic fields.

4. HISTORICAL DATA	DATE	LOCATION
a. CONCEPTION	Feb. 2, 1988	UCSB
b. DISCLOSURE TO OTHERS	Mar.28, 1988	"
c. FIRST SKETCH OR DRAWING	Mar. 28, 1988	"
d. FIRST WRITTEN DESCRIPTION	Mar. 28, 1988	"
e. COMPLETION OF MODEL OR FULL-SIZED DEVICE		
f. FIRST TEST OR OPERATION		

5. NAMES OF PERSONS ACQUAINTED WITH THIS WORK

6. RESULTS OF TEST

7. APPLICATIONS (INDUSTRIAL, GOVERNMENTAL, OTHERS) For use as local oscillator for submillimeter wave spectroscopy of atmosphere - NASA, for military surveillance - DoD

8. REFERENCE REPORTS, PUBLICATIONS AND DRAWINGS

9. JPL CHARGE NO. 215-2EP02-0-3460

10. NASA TASK ORDER NO. RE-238

11. SIGNATURES

TECHNOLOGY UTILIZATION STAFF MEMBER	INNOVATOR(S)	DATE REPORTED
Robert D. Jarvis	(1) J Maserjian	11-15-88
APPROVED Mgr Office of Patent Counsel Luther P. Speck	(2)	
APPROVED Mgr Patents and Tech Utilization Howard B. Scheckman	(3)	
	(4)	

Jet Propulsion Laboratory

N E W T E C H N O L O G Y R E P O R T

JPL & NASA Case No. NPO-17754

JPL Log No. 7256

TUNABLE SUBMILLIMETER WAVE GENERATOR

I. The Novelty

A very high frequency local oscillator for heterodyne mixing comprises a plurality of parabolic quantum wells with energy levels resembling harmonic oscillator devices, wherein an electron current is introduced among the wells thereby accelerating the electrons into higher energy levels such that they emit monochromatic submillimeter wave radiation corresponding to transitions between the energy levels in a manner analogous to cyclotron emission without high magnetic fields.

II. The Disclosure

The Problem

There exists a critical need for efficient local oscillators for heterodyne mixers operating in the 300 to 3000 GHz region. Applications include space-based submillimeter wave imaging arrays, airborne atmospheric spectroscopy, all-weather imaging radar, non-destructive testing, plasma diagnostics, weapon and contraband detection, and communications.

Such local oscillators must have reasonable power (in the range of milliwatts up to watts) and are required to cover a wide spectral range. Lasers developed for this purpose are (individually) restricted to essentially one single wavelength. Some tunability can be achieved by optical techniques, but only over very limited bandwidths. Microwave generators, such as carcinotrons, do not operate efficiently at wavelengths shorter than one millimeter, and are excessively heavy,

consume considerable power, and have short lifetimes, restricting their use in flight missions.

Available solid state oscillators, such as GaAs Gunn diodes, and IMPATTs, are highly efficient and tunable, but are limited to frequencies up to about 75 and 150 GHz, respectively. Likewise, recent research on quantum well negative differential resistance oscillators projects to only comparable power-frequency performance. Higher frequencies can be achieved by generating harmonics of the solid state oscillator frequencies using solid state nonlinear devices such as GaAs varactors or varistors. This approach is limited by the reduced power output at the higher harmonic frequencies. This latter limiitation is being partially overcome by developing device arrays to increase the total power output (Ref. 1,2). Ultimately, the device cut-off frequency will still limit this approach to frequencies not much greater than 1000 GHz.

The Solution

The solution is to use parabolic quantum wells with harmonic oscillator-like energy levels.

Description and Explanation

The concept of this proposal offers the potential of highly efficient solid state oscillators that are tunable over the entire subillimeter wavelength spectrum and beyond. The concept is related to earlier work (Ref. 3) which showed that such radiation can be generated by passing a current in a 2D electron gas of a heterojunction. Two types of emission processes have been demonstrated: The first process is a single particle excitation due to radiative transitions between Landau levels in a magnetic field called cyclotron emission. The second process is the radiative decay of collective 2D plasma oscillations. In this case a grating structure is required next to the 2D

electron gas to couple out the radiation. Although of scientific interest, the above processes are not likely to lead to efficient local oscillators for mixers.

We propose using parabolic quantum wells with harmonic oscillator-like energy levels such as shown in Fig. 1a. Such parabolic quantum wells have been grown (Ref. 4) by molecular-beam-epitaxy (MBE) with appropriate grading of the Al composition of (Al,Ga)As. By introducing an electron current along these quantum wells, the electrons can be accelerated into the higher levels and emit monochromatic submillimeter wave radiation corresponding to transitions between the levels. This process would be analogous to cyclotron emission but without the need for a high magnetic field.

The parabolic quantum well (in the conduction band) contains energy levels

$$E_n = (n-1/2)\,\hbar\omega_0 , \qquad (1)$$

where n = 1,2,3,etc. and

$$\omega_0 = \sqrt{(K/m^*)} , \qquad (2)$$

with m* the electron effective mass and K equal to the curvature of the parabolic well. From Eq. (1) the transitions corresponds to the energy level difference $\hbar\omega_0$. We can predetermine this emission energy by choosing K [see Eq.(2)] -- determined by appropriately grading the Al composition in the well.

In order to provide a tunable oscillator, we further propose grading the value of K. A convenient choice is to vary K by varying the potential of the well U exponentially, as depicted in Fig. 1b and expressed by

$$U = W[\,e^{-z/a} + (z/b)(1-e^{-b/a})] \qquad (3)$$
$$\approx W(\,e^{-z/a} + z/b\,), \qquad b/a \gg 1.$$

This well potential gives a value of K (equal to d^2U/dz^2) at the potential minimum of the well which varies linearly with applied field F ; that is

$$K(F) = (W/b - F)/a . \qquad (4)$$

Since the electrons will populate states at the minimum well potential, they will be excited into the transitions $\hbar\omega_0$ corresponding to the value of K given by Eq. (4), and can thus be tuned by adjusting the field accordingly.

If a large sheet density of electrons n_s is introduced into the well, the electron space charge will flatten the potential at the bottom of the well by a width Δz given by

$$\Delta z = en_s/\epsilon K \qquad (5)$$

where e is the electron charge and ϵ is the well permittivity. This effect will cause a shift in the emission frequency at high injection levels of n_s due to the barrier assymmetry. This may ultimately limit the maximum value of n_s and thus the maximum power output per quantum well. However, multiple quantum wells can be provided for increased total power output.

For a tunable range of from 300 to 3000 GHz, typical values of well potential parameters might be a = 250 Å, b = 1800 Å, and W = 0.5 eV. The maximum applied fields required with these parameters is 27.5 KV/cm and -7.5 KV/cm corresponding to the frequencies of 300 and 3000 GHz, respectively. These values of fields fall well within normal device operating limits.

Figure 2 illustrates the band diagram of a possible device configuration consisting of two exponential wells with a field applied. The field is obtained by applying a voltage bias V_g accross the total (Al,Ga)As region of thickness d, giving

$$F = V_g/d . \qquad (7)$$

The substrate is doped n+ to provide contact to the underside of the barrier/quantum well layers.

Figure 3 illustrates a possible device stucture, again with just two wells. The Al composition x of the $Al_xGa_{1-x}As$ layers (AlGaAs in the figure) is typically about 0.4 in the barrier layers and graded to appropriately lower values in the exponential wells. The heavily doped N+ regions in the AlGaAs provide a means for injecting electrons into the wells. Al contacts are provided to the source, common gate-drain, and back contact as shown. The

voltage V_g is applied to the common gate-drain contact to determine the field given by Eq.(7) and thus the emission frequency, by Eqs. (2)and (4). The voltage V_g+V_s is applied at the source to inject electrons into the wells with a current (and electron heating) sufficient for the desired emission output, but without excessive linewidth broadening. Again, more wells could be added to increase the output power.

The emission will radiate outward along the plane of the quantum wells. It can be collected or focused with conventional quasi-optical antennas or reflectors. By placing the device inside a cavity with appropriate reflectors, and if there is sufficient gain through stimulated emission, it may also be possible to achieve laser action. The device would then perform as a laser which could be tuned through the numerous cavity modes over a wide spectral range.

References

1. W. W. Lam, C.F. Jou, N. C. Luhmann,Jr., and D. B. Rutledge,"Diode Grids for Electronic Beam Steering and Frequency Multiplication",Int. Journal of Infrared and Millimeter Waves 7, 27 (1986).
2. R. J. Hwu, C. F. Jou, W. W. Lam, B. Hancock, U. Lieneweg, N. C. Luhmann, Jr., J. Maserjian, and D. B. Rutledge, "Watt-Level Millimeter-Wave Monolithic Diode-Grid Frequency Multipliers", 1988 IEEE MTT-S International Microwave Symposium, New York, May 1988; to be published in symposium Digest.
3. R. Hopfel,G. Lindemann, E. Gornik, G. Stangl, A. C. Gossard, and W. Wiegmann, "Cyclotron And Plasmon Emission from Two-Dimensional Electrons in GaAs", Surface Science 113, 118 (1982).
4. R. C. Miller, A. C. Gossard, D. A. Kleinman, and O. Munteanu, "Parabolic Quantum Wells with the GaAs-$Al_xGa_{1-x}As$ System", Phys. Rev. B 29, 3740,(1984).

TUNABLE SUBMILLIMETER WAVE GENERATOR

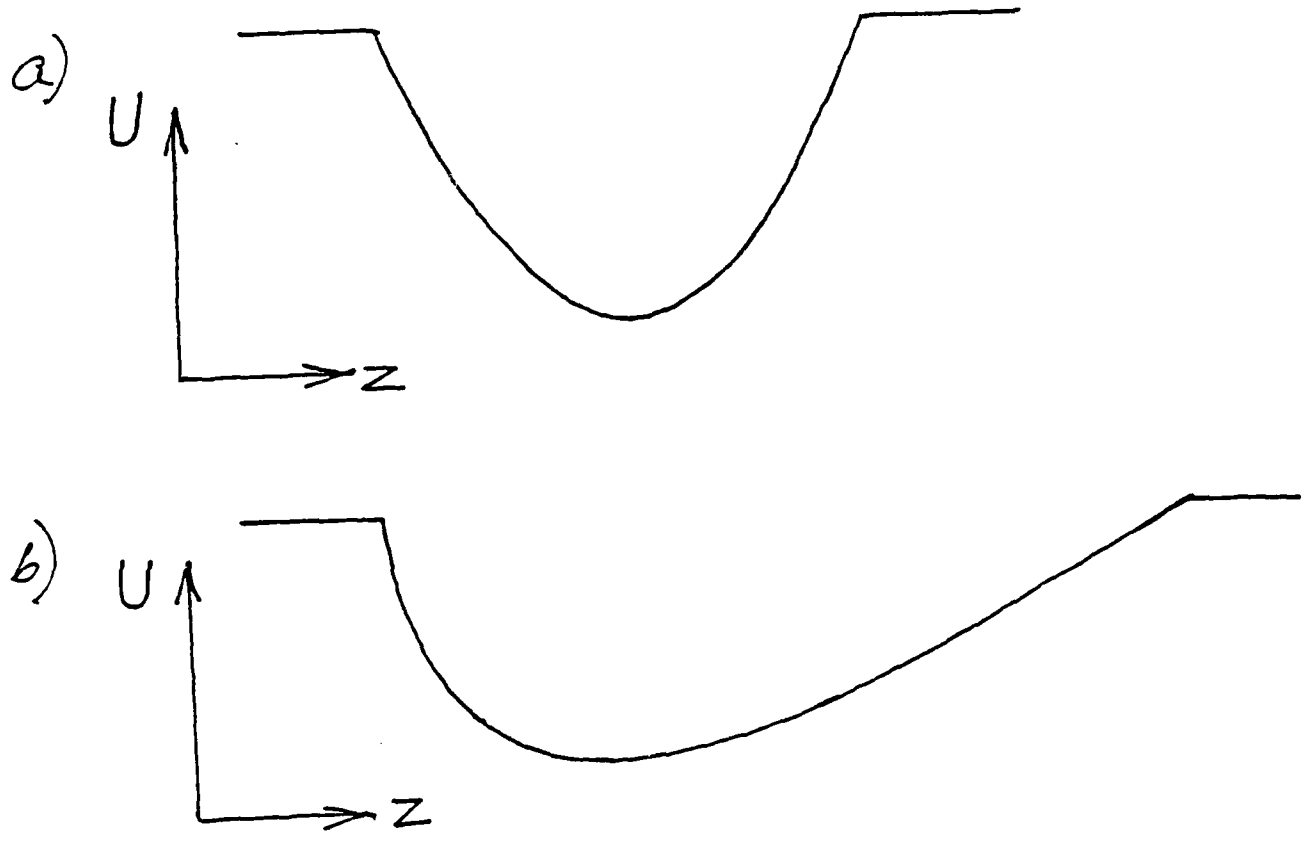

Fig. 1. a) Parabolic well
b) Exponential well

TUNABLE SUBMILLIMETER WAVE GENERATOR

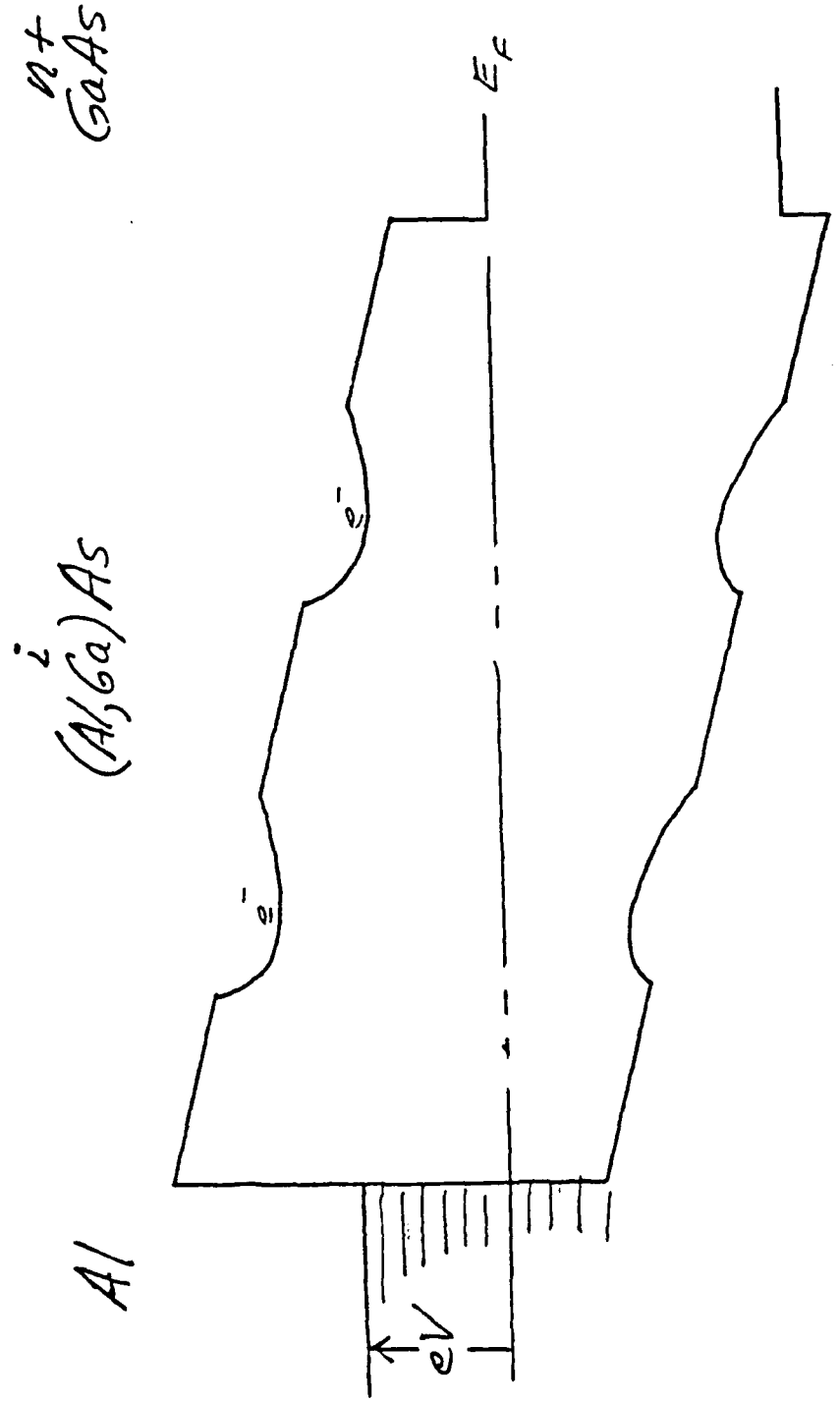

Fig. 2 Band diagram of possible 2-well device structure with voltage bias

TUNABLE SUBMILLIMETER WAVE GENERATOR

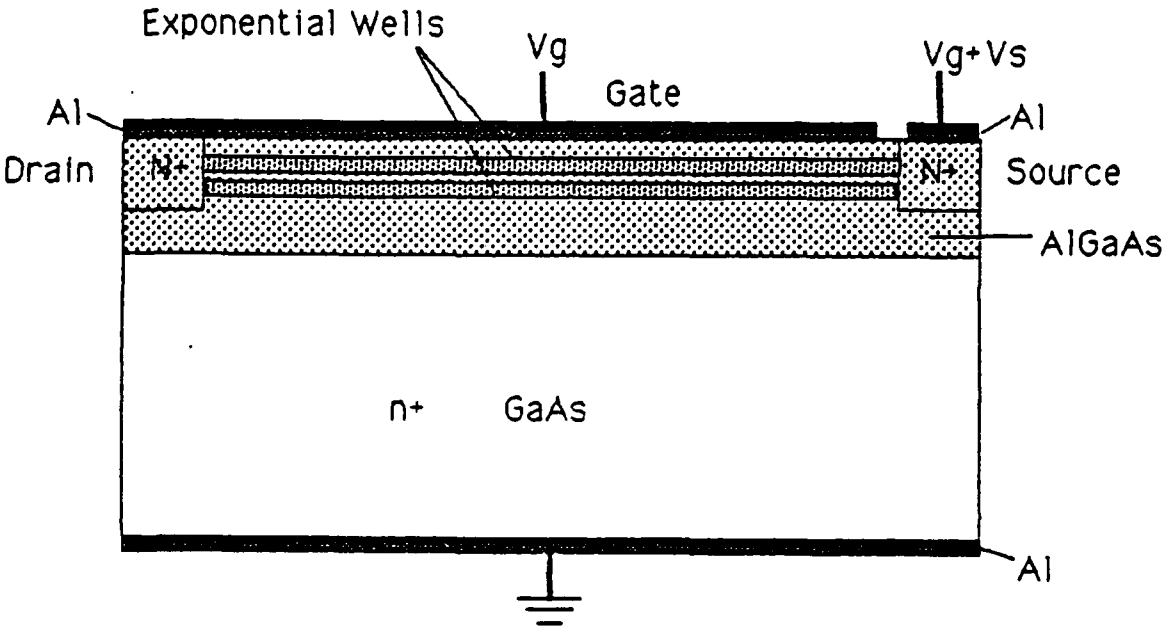

Fig. 3. Cross section of possible device structure
(not to scale)